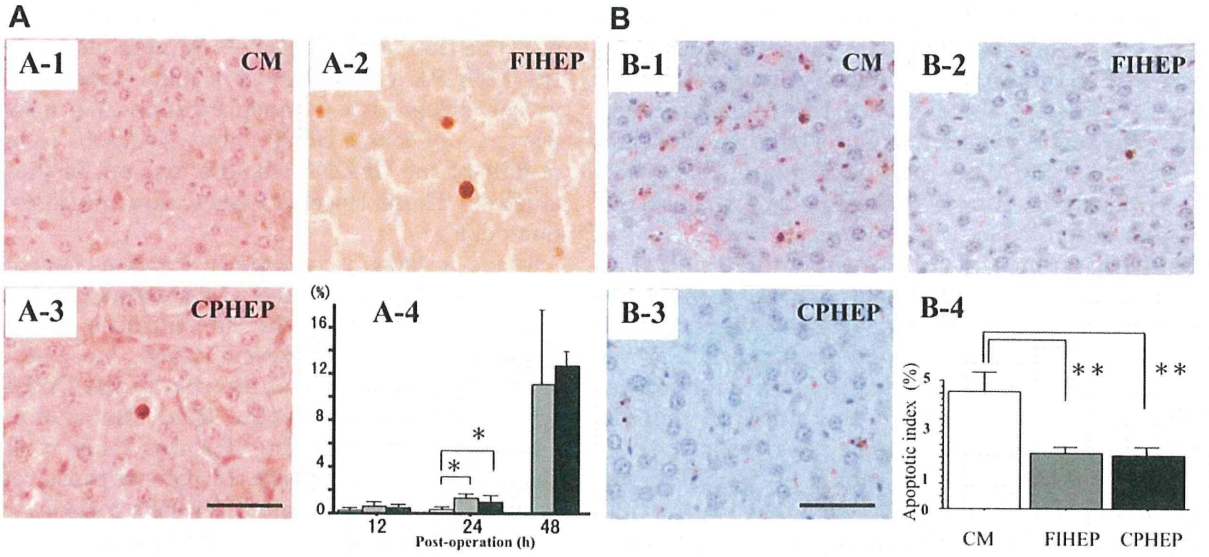

FIG. 5. (A) BrdU-labeling index of hepatocytes in the remnant liver of the hepatocyte- transplanted rat. The rats were injected with CM, transplanted with FIHEPs or CPHEPs, and subjected to ALF as in Fig. 2. The remnant livers (omental lobe) were removed at 12, 24, and 48 h post-induction of ALF and processed to obtain paraffin sections for BrdU staining. (A-1), (A-2), and (A-3) are representative of photos from rats with CM, FIHEPs, and CPHEPs, respectively, taken at 24 h post-ALF. $BrdU^+$ nuclei are brown in color. In (A-4), $BrdU^+$ cells were counted from five microscopic fields of each section from 4 rats in each group at the time points indicated, and the BrdU-labeling index was calculated as the ratio of $BrdU^+$ cells to the total cells in a counted field. The open bar, gray bar, and black bar indicate the CM, FIHEP, and CPHEP groups, respectively. $*P < 0.05$ *versus* the CM group. Bar, 50 μm. (B) Suppression of remnant hepatocyte apoptosis by hepatocyte transplantation. The rats were transplanted with hepatocytes and subjected to ALF as described in Fig. 2. Paraffin sections were prepared from the remnant livers (omental lobes) isolated from the CM (B-1), FIHEP (B-2), and CPHEP groups (B-3) at 24 h post-ALF and were stained for TUNEL activity. $TUNEL^+$ pycnotic nuclei (brown) were frequently observed in the CM group, but less often in the FIHEP and CPHEP groups. Apoptotic cells were counted from five microscopic fields of liver tissue sections from four rats in each group. The ratio of apoptotic cells to total cells in the counted field was expressed as the apoptotic index (B-4). The open bar, gray bar, and black bar indicate the CM, FIHEP, and CPHEP groups, respectively. $**P < 0.01$ *versus* the CM group. Bar, 50 μm.

of the remnant liver in the FIHEP and CPHEP groups decreased to approximately 50% of that in the CM group. These $TUNEL^+$ hepatocytes were host hepatocytes because they were $DPPIV^-$. Thus, CPHEP transplantation suppressed the apoptotic changes in the host hepatocytes as effectively as FIHEP transplantation.

DISCUSSION

Although several studies have supported the effectiveness of hepatocyte transplantation in treating patients with ALF, there is a severe problem in using hepatocyte transplantation therapy as a general clinical treatment for patients with liver failure: owing to the lack of donor organs available for clinical use, hospitals cannot supply sufficient quantities of normal human hepatocytes to such patients. One way to overcome this limitation might be to devise a method of abundantly propagating hepatocytes in culture, starting with a small amount of hepatocytes isolated from small pieces of available liver tissues. However, it does not seem to be a practical solution, because it is well documented that normal hepatocytes show poor multiplication ability *in vitro* despite their remarkable growth potential *in vivo* [19].

We have been engaged in developing a technology to abundantly propagate hepatocytes in culture [8, 9] and previously reported that rat hepatocytes were capable of repeatedly multiplying *in vitro* when cocultured with Swiss 3T3 cells in a medium that we devised [10]. We have now shown that such CPHEPs can be used as a source of hepatocyte transplantation for preventing hepatectomy-induced ALF. Resection of hepatic tumors is currently the gold standard treatment for patients with either primary or secondary liver malignancies. An extended hepatectomy is often necessary to achieve curative resection; however, ALF after massive hepatectomy remains a challenging problem (i.e., the risk of insufficiency of remnant liver volume, leading to unresectability). If we devise a countermeasure to prevent ALF beforehand, aggressive hepatic resection could be safely performed. Seeking to answer this clinical question, we evaluated the prevention efficacy of CPHEP transplantation in a surgical model of hepatectomy-induced ALF.

To estimate the efficacy of transplanting either FIHEPs or CPHEPs in ALF, we employed an experimental ALF model induced by subjecting rats to two-thirds-hepatectomy and ligation of the right-lobe pedicle. This method induces more severe liver failure than

a model induced by 90% hepatectomy and is considered to mimic the clinical status of human ALF fairly faithfully [14]. The rats lacked a functional liver and showed ischemic changes in the right lobe, resulting in regeneration failure of the remnant omental lobe, whose weight occupied about 8% of the total liver weight. This model has previously been used to demonstrate that FIHEP transplantation effectively prolongs the survival of rats suffering from ALF [15]. We reproduced similar results in the present study. Notably, CPHEPs, which had been prepared by multiplying FIHEPs 3 times, were as effective as FIHEPs in prolonging the survival of rats suffering from ALF. CPHEP transplantation improved all the liver functions tested in this study. In addition, the BrdU-labeling index of the hepatocytes in the remnant liver was comparable to that in the FIHEP group. Rats with CPHEPs gradually regained liver weight after ALF induction, as did those with FIHEPs. These results together indicate that both CPHEP and FIHEP could be a source for hepatocyte transplantation to promote regeneration of the remnant liver after ALF induction.

There have been two explanations for lethal hepatic failure after excessive hepatectomy: hepatectomy causes microcircular disturbances [20] or induces cytotoxic factors such as TNF-α, TGF-β1, and oxidative stress-related factors [21, 22]. In the present study, we did not find any evidence of microvascular disturbances on hematoxylin and eosin (H&E)-stained sections of the remnant lobe in the ALF-induced rats, but we did observe hypercytokinemia of cytokines such as IL-6 and TGF-β1. Apoptotic hepatocytes were frequently seen by TUNEL assay in the remnant liver lobe of the ALF-induced rats. CPHEP and FIHEP transplantation decreased the concentrations of IL-6 and TGF-β1 in sera, as well as the frequency of apoptotic hepatocytes. Therefore, it appears that both CPHEPs and FIHEPs prolonged the survival of ALF-induced rats by suppressing the hepatocytic apoptosis in the remnant liver.

In the present study, we demonstrated the presence of DPPIV$^+$ hepatocytes in the spleen at 24 h after ALF induction, which clearly indicated the engraftment of both transplanted CPHEPs and FIHEPs in the graft site. There were no significant differences in the frequency of DPPIV$^+$ hepatocytes between the FIHEP and CPHEP groups. However, the expression level of hepatocyte-specific mRNAs such as Alb, CYP2C7, and GS in the spleen of the CPHEP rats was considerably lower than that in the FIHEP rats. This might be explained by the fact that CPHEPs showed lower expression levels of these marker genes than FIHEPs at the time of transplantation; this was due to the fact that the CPHEP cells had been cultured for 11 d before transplantation, during which time the expression levels had decreased (Fig. 1B). Another explanation could be that the CPHEPs were more vulnerable than the FIHEPs, and that most of them became nonviable in the spleen after transplantation. We noticed the presence of many DPPIV$^+$ but Hoechst$^-$ cells in the middle of the CPHEP clusters, but not in the FIHEP clusters. These Hoechst$^-$ cells were considered to be nonviable.

It has previously been shown that homogenized hepatocytes were even effective as a treatment for liver failure [23], suggesting the effectiveness of nonviable hepatocytes. In the present study, we also showed that the survival rate of the rats in the DHEP group was better, to some extent, than that in the control CM group, although the rate was much lower than that of the CPHEP group. In light of these results, it is likely that transplanted CPHEPs contribute to the improvement of liver failure by substituting the function of the host liver. They may also provide some growth factors or enzymes to support the regeneration of the remnant liver. It remained to be elucidated whether the cryopreserved CPHEPs also display such beneficial effects. Hepatocytes are known to be very sensitive to freezing damage. Three distinct modes of cryopreservation-induced hepatocyte death have been identified, namely, physical cell rupture, necrosis, and apoptosis [24]. The susceptibility of hepatocytes to such freeze-thaw injury is attributed to the damage to mitochondria, including loss of mitochondrial membrane integrity, increase in membrane permeability, etc. The inhibition of mitochondria damage, for instance, by broad-spectrum caspase-inhibitor, would prevent cryopreservation-induced damage of propagated hepatocytes.

In conclusion, the transplantation of homologous CPHEPs has a remarkable therapeutic potential for ALF in rats. Since we have recently established a culture method that enables us to multiply human hepatocytes 50 to 100 times during 50 d of culture [25], CPHEPs might be a useful source of hepatocytes for transplantation to treat human patients with ALF.

REFERENCES

1. Lee WM. Acute liver failure. N Engl J Med 1993;329:1862.
2. Bismuth H, Samuel D, Casting D, et al. Orthotopic liver transplantation in fulminant and subfulminant hepatitis. Ann Surg 1995;222:109.
3. Moreno GE, Garcia GI, Loinaz SC, et al. Liver transplantation in patients with fulminant hepatic failure. Br J Surg 1995;82:118.
4. Gewartowska M, Olszewski WL. Hepatocyte transplantation-biology and application. Ann Transplant 2007;12:27.
5. Habibullah MC, Syde HI, Qamar A, et al. Human fetal hepatocyte transplantation in patients with fulminant hepatic failure. Transplantation 1994;58:951.
6. Strom SC, Fisher RA, Thompson MT, et al. Hepatocyte transplantation as a bridge to orthotopic liver transplantation in terminal liver failure. Transplantation 1997;63:559.

7. Fisher RA, Bu D, Thompson M, et al. Defining hepatocellular chimerism in liver failure patient bridge with hepatocyte infusion. Transplantation 2000;69:303.
8. Tateno C, Yoshizato K. Long-term cultivation of adult rat hepatocytes that undergo multiple cell divisions and express normal parenchymal phenotypes. Am J Pathol 1996;148:383.
9. Tateno C, Takai-Kajihara K, Yamasaki C, et al. Heterogeneity of growth potential of adult rat hepatocytes *in vitro*. Hepatology 2000;31:65.
10. Sato H, Funahashi M, Kristensen DB, et al. Pleiotrophin as a Swiss 3T3 cell-derived potent mitogen for adult rat hepatocytes. Exp Cell Res 1999;246:152.
11. Hino H, Tateno C, Sato H, et al. A long-term culture of human hepatocytes which show a high growth potential and express their differentiated phenotypes. Biochem Biophys Res Commun 1999;256:184.
12. Seglen PO. Preparation of isolated rat liver cells. Methods Cell Biol 1976;13:29.
13. Katayama S, Tateno C, Asahara T, et al. Size-dependent *in vivo* growth potential of adult rat hepatocytes. Am J Pathol 2001; 158:97.
14. Eguchi S, Lilja H, Hewitt W, et al. Loss and recovery of liver regeneration in rats with fulminant hepatic failure. J Surg Res 1997;72:112.
15. Eguchi S, Kamolt A, Ljubiova J, et al. Fulminant hepatic failure in rats: Survival and effects on blood chemistry and liver regeneration. Hepatology 1996;24:1452.
16. Higgins GM, Anderson RM. Experimental pathology of the liver. 1. Restoration of the liver of the white rat following partial surgical removal. Arch Pathol 1931;12:186.
17. Gordon GJ, Coleman WB, Hixon DC, et al. Liver regeneration in rats with retrosine-induced hepatocellular injury proceeds through a novel cellular response. Am J Pathol 2000; 156:607.
18. Asahina K, Sato H, Yamasaki C, et al. Pleiotrophin/heparin-binding growth-associated molecule as a mitogen of rat hepatocytes and its role in regeneration and development of liver. Am J Pathol 2002;160:2191.
19. Fausto N, Campbell JS, Riehle KJ. Liver regeneration. Hepatology 2006;43(2 Suppl. 1):45.
20. Kamimukai N, Togo S, Hasegawa S, et al. Expression of Bcl-2 family reduces apoptotic hepatocytes after excessive hepatectomy. Eur Surg Res 2001;33:8.
21. Leist M, Gantner F, Bohlinger I, et al. Tumor necrosis factor-induced hepatocyte apoptosis precedes liver failure in experimental murine shock models. Am J Pathol 1995;146:1220.
22. Oberhammer FA, Pavelka M, Sharma S, et al. Induction of apoptosis in culture hepatocytes and in regressing liver by transforming growth factor β1. Proc Natl Acad Sci U S A 1992; 89:5408.
23. Grundmann R, Koebe HG, Waters W. Transplantation of cryopreserved hepatocytes or liver cytosol injection in the treatment of acute liver failure in rats. Res Exp Med 1986; 186:141.
24. Terry C, Dhawan A, Mitry RR, Hughes RD. Cryopreservation of isolated human hepatocytes for transplantation: State of the art. Cryobiology 2006;53:149.
25. Yamasaki C, Tateno C, Aratani A, et al. Growth and differentiation of colony-forming human hepatocytes in vitro. J Hepatol 2006;44:749.

Journal of Virology

Hepatitis C Virus Hijacks P-Body and Stress Granule Components around Lipid Droplets

Yasuo Ariumi, Misao Kuroki, Yukihiro Kushima, Kanae Osugi, Makoto Hijikata, Masatoshi Maki, Masanori Ikeda and Nobuyuki Kato

J. Virol. 2011, 85(14):6882. DOI: 10.1128/JVI.02418-10.
Published Ahead of Print 4 May 2011.

JOURNAL OF VIROLOGY, July 2011, p. 6882–6892 Vol. 85, No. 14
0022-538X/11/$12.00 doi:10.1128/JVI.02418-10

Hepatitis C Virus Hijacks P-Body and Stress Granule Components around Lipid Droplets[▽]

Yasuo Ariumi,[1,2]* Misao Kuroki,[1] Yukihiro Kushima,[3] Kanae Osugi,[4] Makoto Hijikata,[3] Masatoshi Maki,[4] Masanori Ikeda,[1] and Nobuyuki Kato[1]

Department of Tumor Virology, Okayama University Graduate School of Medicine, Dentistry, and Pharmaceutical Sciences, Okayama 700-8558, Japan[1]; Center for AIDS Research, Kumamoto University, Kumamoto 860-0811, Japan[2]; Department of Viral Oncology, Institute for Virus Research, Kyoto University, Kyoto 606-8507, Japan[3]; and Department of Applied Molecular Biosciences, Graduate School of Bioagricultural Sciences, Nagoya University, Nagoya 464-8601, Japan[4]

Received 19 November 2010/Accepted 21 April 2011

The microRNA miR-122 and DDX6/Rck/p54, a microRNA effector, have been implicated in hepatitis C virus (HCV) replication. In this study, we demonstrated for the first time that HCV-JFH1 infection disrupted processing (P)-body formation of the microRNA effectors DDX6, Lsm1, Xrn1, PATL1, and Ago2, but not the decapping enzyme DCP2, and dynamically redistributed these microRNA effectors to the HCV production factory around lipid droplets in HuH-7-derived RSc cells. Notably, HCV-JFH1 infection also redistributed the stress granule components GTPase-activating protein (SH3 domain)-binding protein 1 (G3BP1), ataxin-2 (ATX2), and poly(A)-binding protein 1 (PABP1) to the HCV production factory. In this regard, we found that the P-body formation of DDX6 began to be disrupted at 36 h postinfection. Consistently, G3BP1 transiently formed stress granules at 36 h postinfection. We then observed the ringlike formation of DDX6 or G3BP1 and colocalization with HCV core after 48 h postinfection, suggesting that the disruption of P-body formation and the hijacking of P-body and stress granule components occur at a late step of HCV infection. Furthermore, HCV infection could suppress stress granule formation in response to heat shock or treatment with arsenite. Importantly, we demonstrate that the accumulation of HCV RNA was significantly suppressed in DDX6, Lsm1, ATX2, and PABP1 knockdown cells after the inoculation of HCV-JFH1, suggesting that the P-body and the stress granule components are required for the HCV life cycle. Altogether, HCV seems to hijack the P-body and the stress granule components for HCV replication.

Hepatitis C virus (HCV) is the causative agent of chronic hepatitis, which progresses to liver cirrhosis and hepatocellular carcinoma. HCV is an enveloped virus with a positive single-stranded 9.6-kb RNA genome, which encodes a large polyprotein precursor of approximately 3,000 amino acid (aa) residues. This polyprotein is cleaved by a combination of the host and viral proteases into at least 10 proteins in the following order: core, envelope 1 (E1), E2, p7, nonstructural 2 (NS2), NS3, NS4A, NS4B, NS5A, and NS5B (12, 13, 21). The HCV core protein, a nucleocapsid, is targeted to lipid droplets (LDs), and the dimerization of the core protein by a disulfide bond is essential for the production of infectious virus (24). Recently, LDs have been found to be involved in an important cytoplasmic organelle for HCV production (26). Budding is an essential step in the life cycle of enveloped viruses. The endosomal sorting complex required for transport (ESCRT) system has been involved in such enveloped virus budding machineries, including that of HCV (5).

DEAD-box RNA helicases with ATP-dependent RNA-unwinding activities have been implicated in various RNA metabolic processes, including transcription, translation, RNA splicing, RNA transport, and RNA degradation (32). Previously, DDX3 was identified as an HCV core-interacting protein by yeast two-hybrid screening (25, 29, 43). Indeed, DDX3 is required for HCV RNA replication (3, 31). DDX6 (Rck/p54) is also required for HCV replication (16, 33). DDX6 interacts with an initiation factor, eukaryotic initiation factor 4E (eIF-4E), to repress the translational activity of mRNP (38). Furthermore, DDX6 regulates the activity of the decapping enzymes DCP1 and DCP2 and interacts directly with Argonaute-1 (Ago1) and Ago2 in the microRNA (miRNA)-induced silencing complex (miRISC) and is involved in RNA silencing. DDX6 localizes predominantly in the discrete cytoplasmic foci termed the processing (P) body. Thus, the P body seems to be an aggregate of translationally repressed mRNPs associated with the translation repression and mRNA decay machinery.

In addition to the P body, eukaryotic cells contain another type of RNA granule termed the stress granule (SG) (1, 6, 22, 30). SGs are aggregates of untranslating mRNAs in conjunction with a subset of translation initiation factors (eIF4E, eIF3, eIF4A, eIFG, and poly(A)-binding protein [PABP]), the 40S ribosomal subunits, and several RNA-binding proteins, including PABP, T cell intracellular antigen 1 (TIA-1), TIA-1-related protein (TIAR), and GTPase-activating protein (SH3 domain)-binding protein 1 (G3BP1). SGs regulate mRNA translation and decay as well as proteins involved in various aspects of mRNA metabolisms. SGs are cytoplasmic phase-dense structures that occur in eukaryotic cells exposed to various environmental stress, including heat, arsenite, viral infection, oxidative conditions, UV irradiation, and hypoxia. Impor-

* Corresponding author. Mailing address: Center for AIDS Research, Kumamoto University, 2-2-1 Honjo, Kumamoto 860-0811, Japan. Phone and fax: 81 96 373 6834. E-mail: ariumi@kumamoto-u.ac.jp.
▽ Published ahead of print on 4 May 2011.

tantly, several viruses target SGs and stress granule components for viral replication (10, 11, 34, 39). Recent studies suggest that SGs and the P body physically interact and that mRNAs may move between the two compartments (1, 6, 22, 28, 30).

miRNAs are a class of small noncoding RNA molecules ~21 to 22 nucleotides (nt) in length. miRNAs usually interact with 3′-untranslated regions (UTRs) of target mRNAs, leading to the downregulation of mRNA expression. Notably, the liver-specific and abundant miR-122 interacts with the 5′-UTR of the HCV RNA genome and facilitates HCV replication (15, 17, 19, 20, 31). Ago2 is at least required for the efficient miR-122 regulation of HCV RNA accumulation and translation (40). However, the molecular mechanism(s) for how DDX6 and miR-122 as well as DDX3 positively regulate HCV replication is not fully understood. Therefore, we investigated the potential role of P-body and stress granule components in HCV replication.

MATERIALS AND METHODS

Cell culture. 293FT cells were cultured in Dulbecco's modified Eagle's medium (DMEM; Invitrogen, Carlsbad, CA) supplemented with 10% fetal bovine serum (FBS). HuH-7-derived RSc cured cells, in which cell culture-generated HCV-JFH1 (JFH1 strain of genotype 2a) (37) could infect and effectively replicate, were cultured in DMEM with 10% FBS as described previously (3–5, 23).

Plasmid construction. To construct pcDNA3-FLAG-DDX6, a DNA fragment encoding DDX6 was amplified from total RNAs derived from RSc cells by reverse transcription (RT)-PCR using KOD-Plus DNA polymerase (Toyobo) and the following pairs of primers: 5′-CGGGATCCAAGATGAGCACGGCC AGAACAGAGAACCCTGTT-3′ (forward) and 5′-CCGCTCGAGTTAAGGT TTCTCATCTTCTACAGGCTCGCT-3′ (reverse). The obtained DNA fragments were subcloned into either BamHI-XhoI site of the pcDNA3-FLAG vector (2), and the nucleotide sequences were determined by BigDye termination cycle sequencing using an ABI Prism 310 genetic analyzer (Applied Biosystems, Foster City, CA).

RNA interference. The following small interfering RNAs (siRNAs) were used: human ATXN2/ATX2/ataxin-2 (siGENOME SMRT pool M-011772-01-005), human PABP1/PABPC1 (siGENOME SMRT pool M-019598-01-005), human Lsm1 (siGENOME SMRT pool M-005124-01-005), human Xrn1 (siGENOME SMRT pool M-013754-01-005), human G3BP1 (ON-TARGETplus SMRT pool L-012099-00-005), human PATL1 (siGENOME SMRT pool M-015591-00-005), and siGENOME nontargeting siRNA pool 1 (D-001206-13-05) (Dharmacon, Thermo Fisher Scientific, Waltham, MA), as a control. siRNAs (25 nM final concentration) were transiently transfected into RSc cells (3–5, 23) using Oligofectamine (Invitrogen) according to the manufacturer's instructions. Oligonucleotides with the following sense and antisense sequences were used for the cloning of short hairpin RNA (shRNA)-encoding sequences targeted to DDX6 (DDX6i) as well as the control nontargeting shRNA (shCon) in a lentiviral vector: 5′-GATCC CCGGAGGAACTAACTCTGAAGTTCAAGAGACTTCAGAGTTAGTTCCT CCTTTTTGGAAA-3′ (sense) and 5′-AGCTTTTCCAAAAAGGAGGAACTAA CTCTGAAGTCTCTTGAACTTCAGAGTTAGTTCCTCCGGG-3′ (antisense) for DDX6i and 5′-GATCCCCGAATCCAGAGGTAATCTACTTCAAGAGA GTAGATTACCTCTGGATTCTTTTTGGAAA-3′ (sense) and 5′-AGCTTTTC CAAAAAGAATCCAGAGGTAATCTACTCTCTTGAAGTAGATTACCTC TGGATTCGGG-3′ (antisense) for shCon. The oligonucleotides described above were annealed and subcloned into the BglII-HindIII site, downstream from an RNA polymerase III promoter of pSUPER (8), to generate pSUPER-DDX6i and pSUPER-shCon, respectively. To construct pLV-DDX6i and pLV-shCon, the BamHI-SalI fragments of the corresponding pSUPER plasmids were subcloned into the BamHI-SalI site of pRDI292, an HIV-1-derived self-inactivating lentiviral vector containing a puromycin resistance marker allowing for the selection of transduced cells (7). pLV-DDX3i, described previously (3), was used.

Lentiviral vector production. The vesicular stomatitis virus G protein (VSV-G)-pseudotyped HIV-1-based vector system was described previously (27, 44). The lentiviral vector particles were produced by the transient transfection of the second-generation packaging construct pCMV-ΔR8.91 (27, 44), the VSV-G-envelope-expressing plasmid pMDG2, as well as pRDI292 into 293FT cells with FuGene6 reagent (Roche Diagnostics, Mannheim, Germany).

HCV infection experiments. The supernatants were collected from cell culture-generated HCV-JFH1 (37)-infected RSc cells (3–5, 23) at 5 days postinfection and stored at −80°C after filtering through a 0.45-μm filter (Kurabo, Osaka, Japan) until use. For infection experiments with HCV-JFH1, RSc cells (1×10^5 cells/well) were plated onto 6-well plates and cultured for 24 h. We then infected the cells at a multiplicity of infection (MOI) of 1 or 4. The culture supernatants were collected at 24 h postinfection, and the levels of the core protein were determined by an enzyme-linked immunosorbent assay (ELISA) (Mitsubishi Kagaku Bio-Clinical Laboratories, Tokyo, Japan). Total RNA was also isolated from the infected cellular lysates by using an RNeasy minikit (Qiagen, Hilden, Germany) for analysis of intracellular HCV RNA. The infectivity of HCV-JFH1 in the culture supernatants was determined by a focus-forming assay at 48 h postinfection. HCV-JFH1-infected cells were detected by using anti-HCV core (CP-9 and CP-11 mixture).

Quantitative RT-PCR analysis. The quantitative RT-PCR analysis of HCV RNA was performed by real-time LightCycler PCR (Roche) as described previously (3–5, 14, 23). We used the following forward and reverse primer sets for the real-time LightCycler PCR: 5′-ATGAGTCATGTGGCAGTGGA-3′ (forward) and 5′-GCTGGCTGTACTTCCTCCAC-3′ (reverse) for DDX3, 5′-ATG AGCACGGCCAGAACAGA-3′ (forward) and 5′-TTGCTGTGTCTGTGTGC CCC-3′ (reverse) for DDX6, 5′-TGACGGGGTCACCCACACTG-3′ (forward) and 5′-AAGCTGTAGCCGCGCTCGGT-3′ (reverse) for β-actin, and 5′-AGA GCCATAGTGGTCTGCGG-3′ (forward) and 5′-CTTTCGCAACCCAACGC TAC-3′ (reverse) for HCV-JFH1.

Preparation of anti-PATL1 antibody. The anti-PATL1 antiserum was raised in rabbits using the glutathione *S*-transferase (GST)-fused PATL1 Ct (C-terminal region of PATL1, aa 450 to 770) as an antigen, and immunoglobulins were affinity purified by using the maltose-binding protein (MBP)-fused PATL1 Ct that was immobilized on an *N*-hydroxysuccinimide (NHS) column (GE Healthcare Bio-Sciences AB, Uppsala, Sweden).

Preparation of LDs. Lipid droplets (LDs) were prepared as described previously (26). Cells were pelleted by centrifugation at 1,500 rpm. The pellet was resuspended in hypotonic buffer (50 mM HEPES [pH 7.4], 1 mM EDTA, 2 mM $MgCl_2$) supplemented with a protease inhibitor cocktail (Nacalai Tesque, Kyoto, Japan) and was incubated for 10 min at 4°C. The suspension was homogenized with 30 strokes of a glass Dounce homogenizer using a tight-fitting pestle (Wheaton, Millville, NJ). A 1/10 volume of 10× isotonic buffer {0.2 M HEPES (pH 7.4), 1.2 M potassium acetate (KoAc), 40 mM magnesium acetate [$Mg(oAc)_2$], and 50 mM dithiothreitol (DTT)} was added to the homogenate. The nuclei were removed by centrifugation at 2,000 rpm for 10 min at 4°C. The supernatant was collected and centrifuged at 16,000 × *g* for 10 min at 4°C. The supernatant was mixed with an equal volume of 1.04 M sucrose in isotonic buffer (50 mM HEPES, 100 mM KCl, 2 mM $MgCl_2$, and protease inhibitor cocktail). The solution was set in a 13.2-ml Polyallomer centrifuge tube (Beckman Coulter, Brea, CA). One milliliter of isotonic buffer was loaded onto the sucrose mixture. The tube was centrifuged at 100,000 × *g* in an SW41Ti rotor (Beckman Coulter) for 1 h at 4°C. After the centrifugation, the LD fraction on the top of the gradient solution was recovered in phosphate-buffered saline (PBS). The collected LD fraction was used for Western blot analysis.

Western blot analysis. Cells were lysed in a buffer containing 50 mM Tris-HCl (pH 8.0), 150 mM NaCl, 4 mM EDTA, 1% Nonidet P-40, 0.1% sodium dodecyl sulfate (SDS), 1 mM DTT, and 1 mM phenylmethylsulfonyl fluoride. Supernatants from these lysates were subjected to SDS-polyacrylamide gel electrophoresis, followed by immunoblot analysis using anti-DDX3 (catalog no. 54257 [NT] and 5428 [IN]; Anaspec, San Jose, CA), anti-DDX6 (A300-460A; Bethyl Laboratories, Montgomery, TX), anti-adipose differentiation-related protein (ADFP; GTX110204; GeneTex, San Antonio, TX), anti-calnexin (NT; Stressgen, Ann Arbor, MI), anti-HCV core (CP-9 and CP-11; Institute of Immunology, Tokyo, Japan), anti-β-actin antibody (A5441; Sigma, St. Louis, MO), anti-ATX2/SCA2 antibody (A302-033A; Bethyl), anti-PABP (sc-32318 [10E10]; Santa Cruz Biotechnology, Santa Cruz, CA), anti-PABP (ab21060; Abcam, Cambridge, United Kingdom), anti-G3BP1 (611126; BD Transduction Laboratories, San Jose, CA), anti-LSM1 (LS-C97364, Life Span Biosciences, Seattle, WA), anti-HSP70 (610607; BD), anti-XRN1 (A300-443A; Bethyl), or anti-PATL1 antibody.

Immunofluorescence and confocal microscopic analysis. Cells were fixed in 3.6% formaldehyde in PBS, permeabilized in 0.1% NP-40 in PBS at room temperature, and incubated with anti-DDX3 antibody (54257 [NT] and 5428 [IN]; Anaspec), anti-DDX3X (LS-C64576; Life Span), anti-DDX6 (A300-460A; Bethyl), anti-HCV core (CP-9 and CP-11), anti-ATX2/SCA2 antibody (A302-033A; Bethyl), anti-ataxin-2 (611378; BD), anti-PABP (ab21060; Abcam), anti-G3BP1 (A302-033A; Bethyl), anti-LSM1 (LS-C97364; Life Span), anti-XRN1

(A300-443A; Bethyl), anti-Dcp2 (A302-597A; Bethyl), anti-human Ago2 (011-22033; Wako, Osaka, Japan), or anti-PATL1 antibody at a 1:300 dilution in PBS containing 3% bovine serum albumin (BSA) for 30 min at 37°C. The cells were then stained with fluorescein isothiocyanate (FITC)-conjugated anti-rabbit antibody (Jackson ImmunoResearch, West Grove, PA) at a 1:300 dilution in PBS containing BSA for 30 min at 37°C. Lipid droplets and nuclei were stained with borondipyrromethene (BODIPY) 493/503 (Molecular Probes, Invitrogen) and DAPI (4′,6-diamidino-2-phenylindole), respectively, for 15 min at room temperature. Following extensive washing in PBS, the cells were mounted onto slides using a mounting medium of 90% glycerin–10% PBS with 0.01% *p*-phenylenediamine added to reduce fading. Samples were viewed under a confocal laser scanning microscope (LSM510; Zeiss, Jena, Germany).

Statistical analysis. A statistical comparison of the infectivities of HCV in the culture supernatants between the knockdown cells and the control cells was performed by using the Student *t* test. *P* values of less than 0.05 were considered statistically significant. All error bars indicate standard deviations.

RESULTS

HCV infection hijacks the P-body components. To investigate the potential role of P-body components in the HCV life cycle, we first examined the alteration of the subcellular localization of DDX3 or DDX6 by HCV-JFH1 infection using confocal laser scanning microscopy as previously described (2), since both DDX3 and DDX6 were identified previously as P-body components (6). For this, we used HuH-7-derived RSc cells, in which cell culture-generated HCV-JFH1 (JFH1 strain of genotype 2a) (37) can infect and effectively replicate (3, 4, 23). HCV-JFH1-infected RSc cells at 60 h postinfection were stained with anti-HCV core antibody, anti-DDX3, and/or anti-DDX6. Lipid droplets (LDs) and nuclei were stained with BODIPY 493/503 and DAPI (4′,6-diamidino-2-phenylindole), respectively. Samples were viewed under a confocal laser scanning microscope. Although we observed that endogenous DDX3 localized in faint cytoplasmic foci in uninfected RSc cells, DDX3 relocalized, formed ringlike structures, and colocalized with the HCV core protein in response to HCV-JFH1 infection (Fig. 1A). On the other hand, endogenous DDX6 was localized in the evident cytoplasmic foci termed P bodies in the uninfected cells (Fig. 1A). DDX6 also relocalized, formed ringlike structures, and colocalized with the core protein in response to HCV-JFH1 infection (Fig. 1A). Although we failed to observe that most of the P bodies of DDX6 perfectly colocalized with DDX3 in uninfected RSc cells (Fig. 1B), we observed a few P bodies of DDX6 colocalized with DDX3 in the uninfected cells (Fig. 1B, arrowheads). Intriguingly, we found that endogenous DDX3 colocalized with endogenous DDX6 in HCV-JFH1-infected cells (Fig. 1B). To further confirm this finding, pHA-DDX3 (41) and pcDNA3-FLAG-DDX6 were cotransfected into 293FT cells. Consequently, we observed that hemagglutinin (HA)-DDX3 colocalized with FLAG-DDX6 in 293FT cells coexpressing HA-DDX3 and FLAG-DDX6 (Fig. 1B), suggesting cross talk of DDX3 with DDX6. Recently, LDs have been found to be involved in an important cytoplasmic organelle for HCV production (26). Indeed, both DDX3 and DDX6 were recruited around LDs in response to HCV infection, while these proteins did not colocalize with LDs in uninfected naïve RSc cells (Fig. 1C). Furthermore, both DDX3 and DDX6 accumulated in the LD fraction of the HCV-JFH1-infected RSc cells; however, we could not detect both proteins in the LD fraction from uninfected control cells (Fig. 1D), suggesting that DDX3 and DDX6 are recruited around LDs in response to HCV infection.

These results suggest that HCV-JFH1 infection disrupts P-body formation. Therefore, we further examined whether or not HCV-JFH1 disrupts the P-body formations of other microRNA effectors, including Ago2; the Sm-like protein Lsm1, which is a subunit of heptameric-ring Lsm1-7, involved in decapping; the 5′-to-3′ exonuclease Xrn1; the decapping activator PATL1; and the decapping enzyme DCP2 (6, 21, 30). As expected, HCV-JFH1 disrupted the P-body formations of Ago2, Lsm1, and Xrn1 as well as PATL1 (Fig. 2). Lsm1, Xrn1, or PATL1 relocalized, formed ringlike structures, and colocalized with the HCV core protein in response to HCV-JFH1 infection, whereas they were localized predominantly in P bodies in uninfected RSc cells (Fig. 2). In fact, we observed that DDX6 colocalized with Ago2, a P-body marker (Fig. 2). In contrast, HCV-JFH1 failed to disrupt the P-body formation of DCP2 (Fig. 2). Thus, these results suggest that HCV disrupts P-body formation through the hijacking of P-body components.

HCV hijacks stress granule components. Since Nonhoff et al. recently reported that DDX6 interacted with ataxin-2 (ATX2) (28), we examined the potential cross talk among DDX6, ATX2, and HCV. Although ATX2 and G3BP1, a well-known stress granule component (36), were dispersed in the cytoplasm at 37°C, both proteins formed discrete aggregates termed stress granules and colocalized with each other in response to heat shock at 43°C for 45 min, indicating that ATX2 is also stress granule component (Fig. 3A). We did not observe prominent colocalization between DDX6 and ATX2 at 37°C (Fig. 3B). In contrast, we found that DDX6 was recruited, juxtaposed, and partially colocalized with stress granules of ATX2 in response to heat shock at 43°C for 45 min in the uninfected RSc cells (Fig. 3B). Notably, ATX2 was recruited, formed the ring-like structures, and partially colocalized with DDX6 in response to HCV-JFH1 infection even at 37°C (Fig. 3B). Furthermore, we noticed that ATX2 was recruited around LDs in HCV-JFH1-infected cells at 72 h postinfection, while ATX2 did not colocalize with LDs in uninfected cells (Fig. 3C), suggesting the colocalization of ATX2 with the HCV core protein in infected cells. Indeed, ATX2 colocalized with the HCV core protein in HCV-JFH1-infected RSc cells at 37°C (Fig. 3D). Moreover, HCV-JFH1 infection induced the colocalization of the core protein with other stress granule components, G3BP1 or PABP1 as well as ATX2 (Fig. 4 and 5). To further confirm our findings, we examined the time course of the redistribution of DDX6 and G3BP1 after inoculation with HCV-JFH1. Consequently, we still detected the P-body formation of DDX6 and dispersed G3BP1 in the cytoplasm, and we did not observe a colocalization between the HCV core protein and DDX6 at 12 and 24 h postinfection (Fig. 4). In contrast, we found that the P-body formation of DDX6 began to be disrupted at 36 h postinfection (Fig. 4). Consistently, G3BP1 formed stress granules at 36 h postinfection (Fig. 4). We then noticed a ringlike formation of DDX6 or G3BP1 and colocalization with the HCV core protein after 48 h postinfection (Fig. 4), suggesting that the disruption of P-body formation and the hijacking of P-body and stress granule components occur in a late step of HCV infection.

We then examined whether or not HCV-JFH1 infection

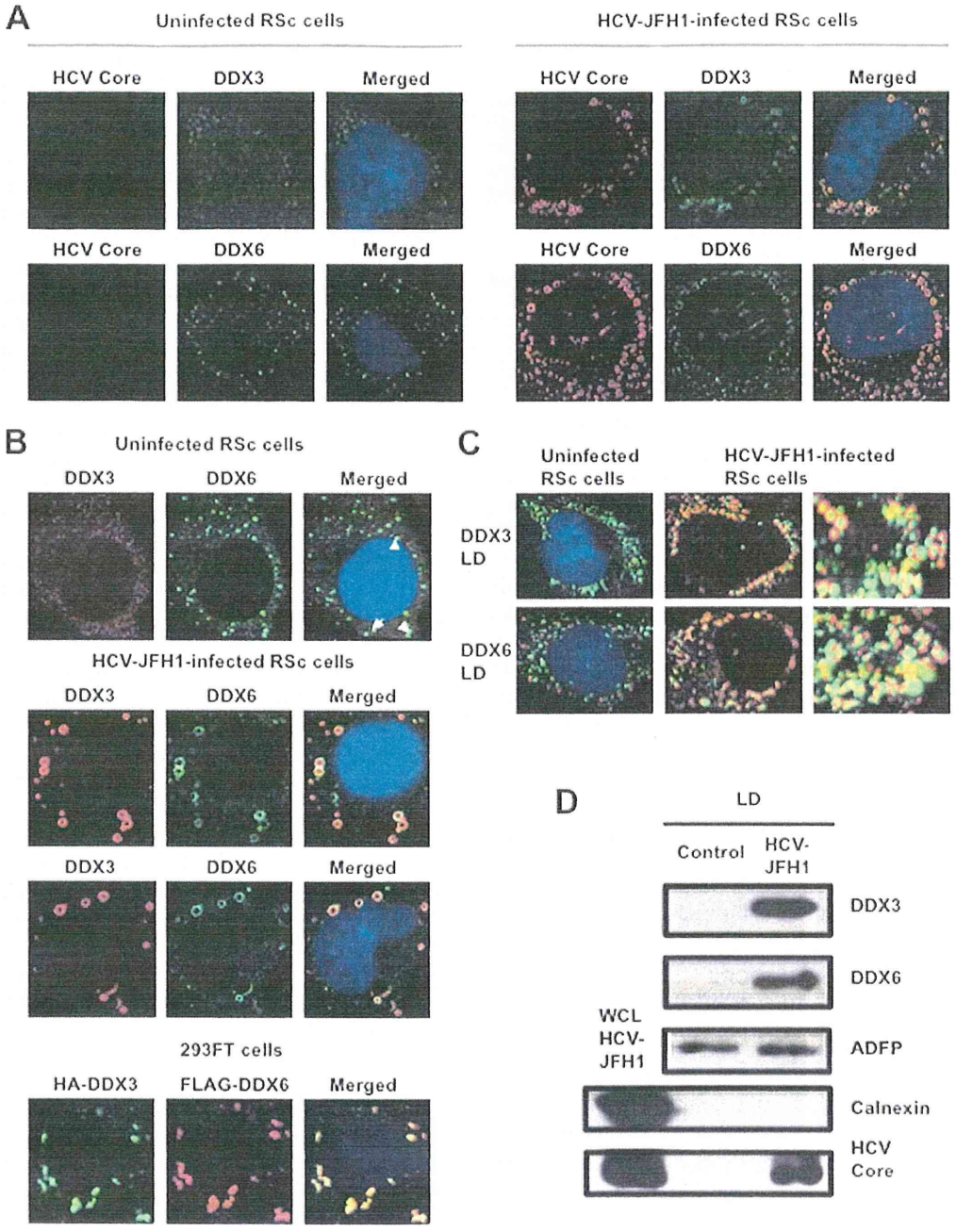

FIG. 1. Dynamic recruitment of DDX3 and DDX6 around lipid droplets (LDs) in response to HCV-JFH1 infection. (A) HCV-JFH1 disrupts the P-body formation of DDX6. Cells were fixed at 60 h postinfection and were then examined by confocal laser scanning microscopy. Cells were stained with anti-HCV core (CP-9 and CP-11 mixture) and either anti-DDX3 (54257 and 54258 mixture) or anti-DDX6 (A300-460A) antibody and then visualized with FITC (DDX3 or DDX6) or Cy3 (core). Images were visualized by using confocal laser scanning microscopy. The two-color overlay images are also exhibited (merged). Colocalization is shown in yellow. (B) HCV-JFH1 recruits DDX3 or DDX6 around LDs. Cells were stained with either anti-DDX3 or anti-DDX6 antibody and were then visualized with Cy3 (red). Lipid droplets and nuclei were stained with BODIPY 493/503 (green) and DAPI (blue), respectively. A high-magnification image is also shown. (C) Colocalization of DDX3 with DDX6. HCV-JFH1-infected RSc cells at 60 h postinfection were stained with anti-DDX3X (LS-C64576) and anti-DDX6 (A300-460A) antibodies. 293FT cells cotransfected with 100 ng of pcDNA3-FLAG-DDX6 and 100 ng of pHA-DDX3 (41) were stained with anti-FLAG-Cy3 and anti-HA-FITC antibodies (Sigma). (D) Association of DDX3 and DDX6 with LDs in response to HCV-JFH1 infection. The LD fraction and whole-cell lysates (WCL) were collected from uninfected RSc cells (control) or HCV-JFH1-infected RSc cells at 5 days postinfection. The results of Western blot analyses of DDX3, DDX6, and the HCV core protein as well as the LD marker ADFP and the endoplasmic reticulum (ER) marker calnexin in the LD fraction are shown.

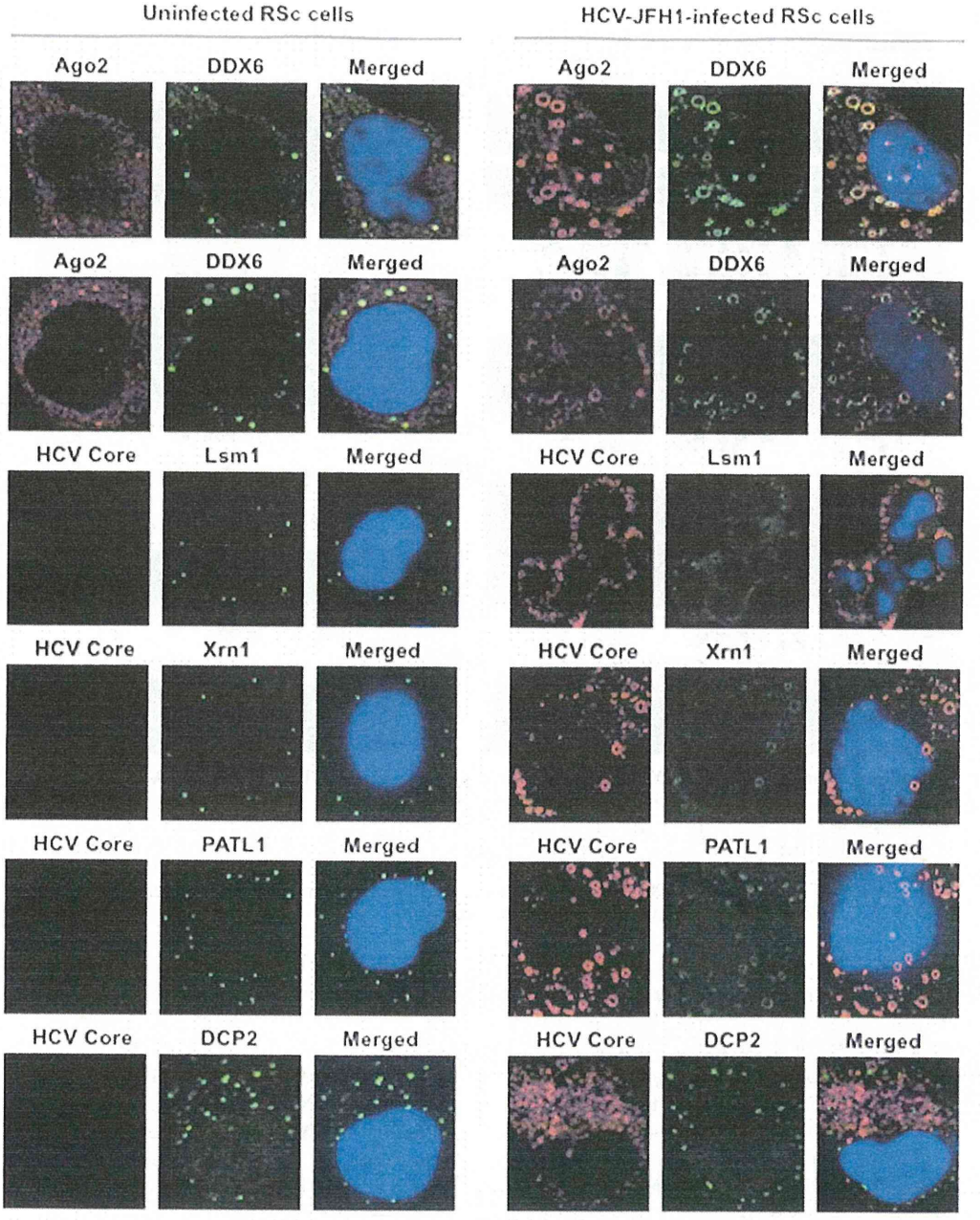

FIG. 2. HCV disrupts the P-body formation of microRNA effectors. Uninfected RSc cells and HCV-JFH1-infected RSc cells at 72 h postinfection were stained with anti-human AGO2 (011-22033) and anti-DDX6 (A300-460A) antibodies. The cells were also stained with anti-HCV core and anti-Lsm1 (LS-C97364), anti-Xrn1 (A300-443A), anti-PATL1, or anti-DCP2 (A302-597A) antibodies and were examined by confocal laser scanning microscopy.

could affect the stress granule formation of G3BP1, ATX2, or PABP1 in response to heat shock or treatment with arsenite. These stress granule components dispersed in the cytoplasm at 37°C, whereas these proteins formed stress granules in response to heat shock at 43°C for 45 min or treatment with 0.5 mM arsenite for 30 min (Fig. 5). In contrast, stress granules were not formed in HCV-JFH1-infected cells at 72 h postinfection in response to heat shock at 43°C for 45 min (Fig. 5), suggesting that HCV-JFH1 infection suppresses stress granule formation in response to heat shock or treatment with arsenite. Intriguingly, G3BP1, ATX2, or PABP1 still colocalized with the HCV core protein even under the above-described stress conditions (Fig. 5). Furthermore, Western blot analysis of cell lysates of uninfected or HCV-JFH1-infected cells at 72 h postinfection showed similar protein expression levels of ATX2, PABP1, HSP70, DDX3, DDX6, and Lsm1 but not G3BP1 (Fig. 6), suggesting that HCV-JFH1 infection does not affect host mRNA translation.

P-body and stress granule components are required for HCV replication. Finally, we investigated the potential role of

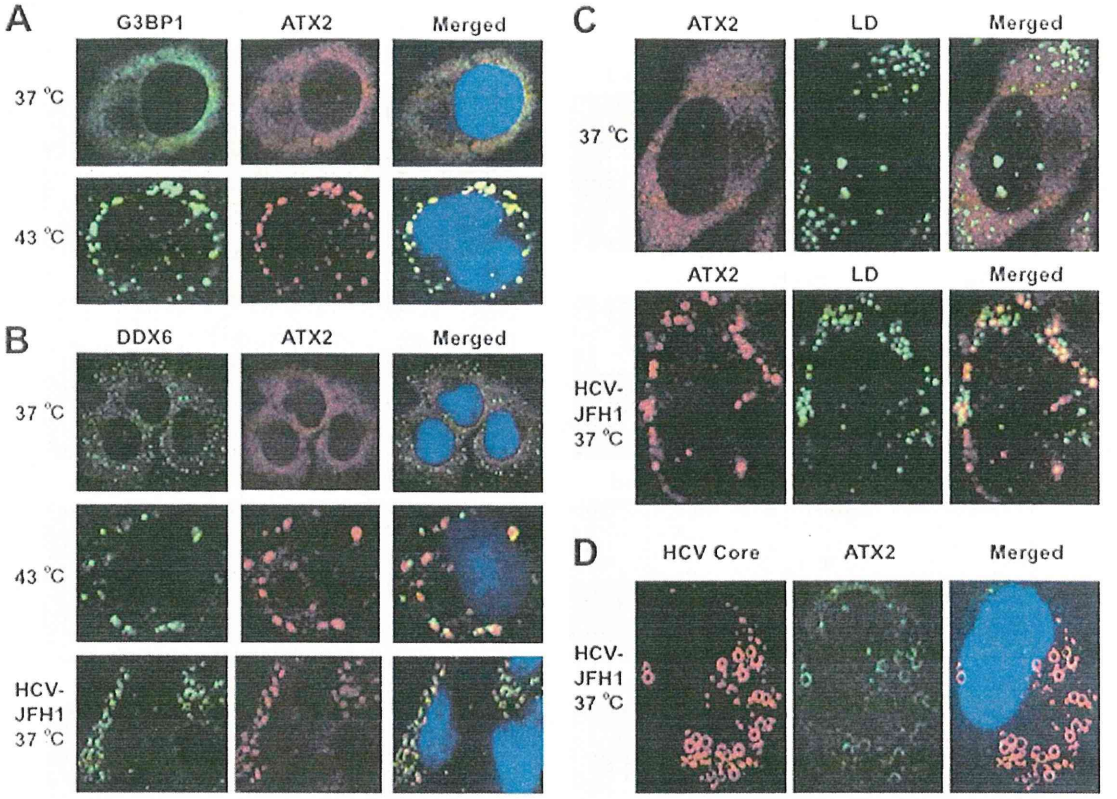

FIG. 3. Dynamic redistribution of ataxin-2 (ATX2) around LDs in response to HCV-JFH1 infection. (A) ATX2 is a stress granule component. RSc cells were incubated at 37°C or 43°C for 45 min. Cells were stained with anti-G3BP1 (A302-033A) and anti-ATX2 (A93520) antibodies and were examined by confocal laser scanning microscopy. (B) Dynamic redistribution of DDX6 and ATX2 in response to heat shock or HCV infection. RSc cells after heat shock at 43°C for 45 min or 72 h after inoculation with HCV-JFH1 were stained with anti-DDX6 and anti-ATX2 (A93520) antibodies. (C) HCV relocalizes ataxin-2 to LDs. HCV-JFH1-infected RSc cells at 72 h postinfection were stained with anti-ATX2 (A93520) antibody and BODIPY 493/503. (D) ATX2 colocalizes with the HCV core protein. HCV-JFH1-infected RSc cells at 72 h postinfection were stained with anti-ATX2/SCA2 (A301-118A) and anti-HCV core antibodies.

P-body and stress granule components in the HCV life cycle. We first used lentiviral vector-mediated RNA interference to stably knock down DDX6 as well as DDX3 in RSc cells. We used puromycin-resistant pooled cells 10 days after lentiviral transduction in all experiments. Real-time LightCycler RT-PCR analysis of DDX3 or DDX6 demonstrated a very effective knockdown of DDX3 or DDX6 in RSc cells transduced with lentiviral vectors expressing the corresponding shRNAs (Fig. 7A). Importantly, shRNAs did not affect cell viabilities (data not shown). We next examined the levels of HCV core and the infectivity of HCV in the culture supernatants as well as the level of intracellular HCV RNA in these knockdown cells 24 h after HCV-JFH1 infection at an MOI of 4. The results showed that the accumulation of HCV RNA was significantly suppressed in DDX3 or DDX6 knockdown cells (Fig. 7B). In this context, the release of the HCV core protein and the infectivity of HCV in the culture supernatants were also significantly suppressed in these knockdown cells (Fig. 7C and D). This finding suggested that DDX6 is required for HCV replication, like DDX3. To further examine the potential role of other P-body and stress granule components in HCV replication, we used RSc cells transiently transfected with a pool of siRNAs specific for ATX2, PABP1, Lsm1, Xrn1, G3BP1, and PATL1 as well as a pool of control siRNAs (siCon) following HCV-JFH1 infection. In spite of the very effective knockdown of each component (Fig. 7E), the siRNAs used in these experiments did not affect cell viabilities (data not shown). Consequently, the accumulation of HCV RNA was significantly suppressed in ATX2, PABP1, or Lsm1 knockdown cells (Fig. 7F), indicting that ATX2, PABP1, and Lsm1 are required for HCV replication. In contrast, the level of HCV RNA was not affected in Xrn1 knockdown cells (Fig. 7F), suggesting that Xrn1 is unrelated to HCV replication. Furthermore, we observed a moderate effect of siG3BP1 and siPATL1 on HCV RNA replication (Fig. 7F). Altogether, HCV seems to hijack the P-body and stress granule components around LDs for HCV replication.

DISCUSSION

So far, the P body and stress granules have been implicated in mRNA translation, RNA silencing, and RNA degradation as well as viral infection (1, 6, 22, 30). Host factors within the P body and stress granules can enhance or limit viral infection, and some viral RNAs and proteins accumulate in the P body and/or stress granules. Indeed, the microRNA effectors DDX6, GW182, Lsm1, and Xrn1 negatively regulate HIV-1 gene expression by preventing the association of viral mRNA

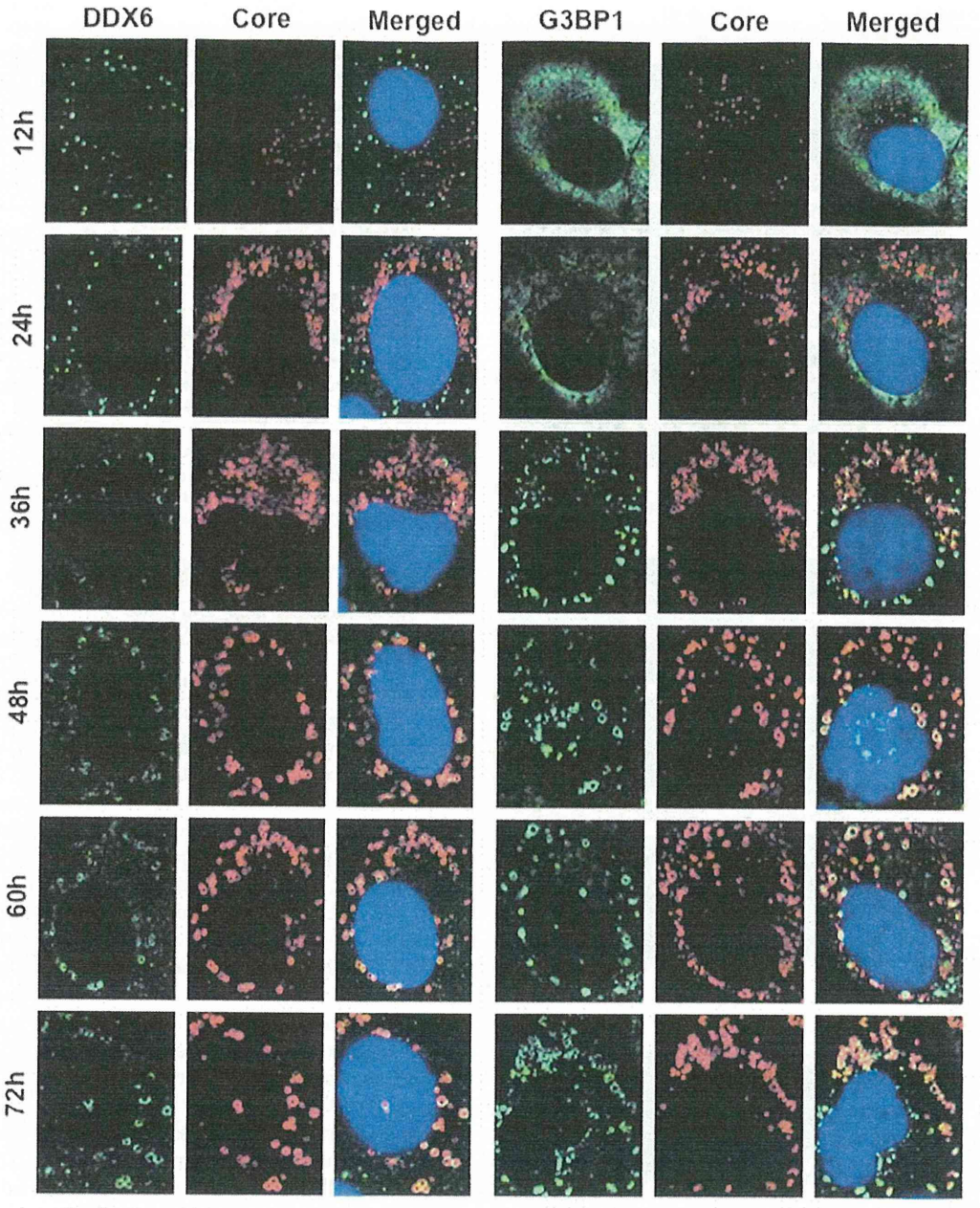

FIG. 4. Dynamic redistribution of DDX6 and G3BP1 in response to HCV-JFH1 infection. RSc cells at the indicated times (hours) after inoculation with HCV-JFH1 were stained with anti-HCV core and either anti-DDX6 (A300-460A) or anti-G3BP1 (A302-033A) antibodies.

with polysomes (9). In contrast, miRNA effectors such as DDX6, Lsm1, PatL1, and Ago2 positively regulate HCV replication (Fig. 7B and F) (16, 31, 33). We have also found that DDX3 and DDX6 are required for HCV RNA replication (3) (Fig. 7B) and that DDX3 colocalized with DDX6 in HCV-JFH1-infected RSc cells (Fig. 1B), suggesting that DDX3 comodulates the DDX6 function in HCV RNA replication. In this regard, the liver-specific miR-122 interacts with the 5′-UTR of the HCV RNA genome and positively regulates HCV replication (15, 17, 19, 20, 31). Since miRNAs usually interact with DDX6 and Ago2 in miRISC and are involved in RNA silencing, DDX6 and Ago2 may be required for miR-122-dependent HCV replication. Indeed, quite recently, a study showed that Ago2 is required for miR-122-dependent HCV RNA replication and translation (40). However, little is known regarding how miR-122 and DDX6 positively regulate HCV replication. Accordingly, we have shown that these miRNA effectors, including DDX6, Lsm1, Xrn1, and Ago2, accumulated around LDs and the HCV production factory and colocalized with the HCV core protein in response to HCV infection (Fig. 1 and 2). However, the decapping enzyme DCP2 did not accumulate and colocalize with the core protein (Fig. 2). Consistent with this finding, Scheller et al. reported previously that the depletion of DCP2 by siRNA did not affect HCV

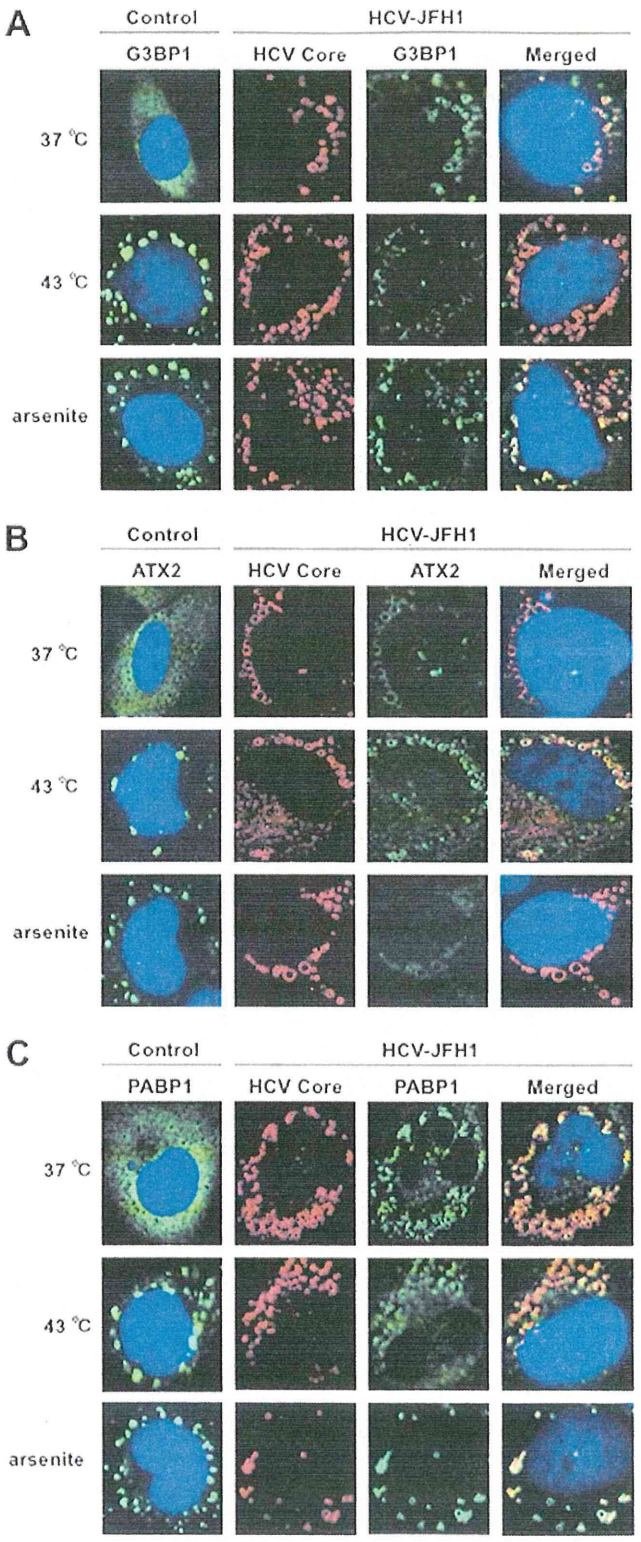

FIG. 5. HCV suppresses stress granule formation in response to heat shock or treatment with arsenite. Naïve RSc cells or HCV-JFH1-infected RSc cells at 72 h postinfection were incubated at 37°C or 43°C for 45 min. Cells were also treated with 0.5 mM arsenite for 30 min. Cells were stained with anti-HCV core and anti-G3BP1 (A), anti-ATX2 (B), or anti-PABP1 (ab21060) (C) antibodies and were examined by confocal laser scanning microscopy.

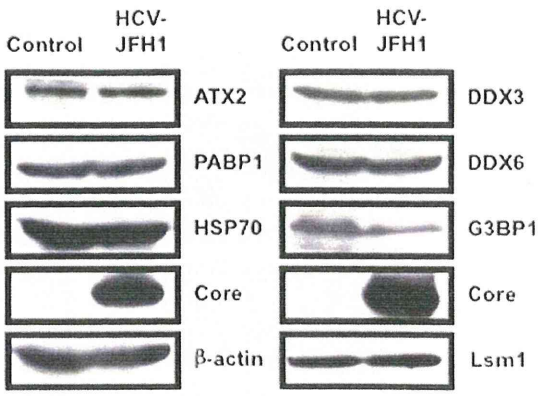

FIG. 6. Host protein expression levels in response to HCV-JFH1 infection. The results of the Western blot analyses of cellular lysates with anti-ATX2/SCA2 antibody (A301-118A), anti-PABP1 (ab21060), anti-HSP70 (610607), anti-HCV core, anti-β-actin, anti-DDX3 (54257 [NT] and 5428 [IN] mixture), anti-DDX6 (A300-460A), anti-G3BP1 (611126), or anti-LSM1 (LS-C97364) antibody in HCV-JFH1-infected RSc cells at 72 h postinfection as well as in naïve RSc cells are shown.

production (33). Since HCV harbors the internal ribosome entry site (IRES) structure in the 5′-UTR of the HCV genome instead of a cap structure, unlike HIV-1, DCP2 may not be recruited on the HCV genome and utilized for HCV replication. Otherwise, DCP2 may determine whether or not DDX6 and miRNAs positively or negatively regulate target mRNA.

Furthermore, we have demonstrated that HCV infection hijacks the P-body and stress granule components around LDs (Fig. 1, 2, 4, and 5). We have found that the P-body formation of DDX6 began to be disrupted at 36 h postinfection (Fig. 4). Consistently, G3BP1 formed stress granules at 36 h postinfection. We then observed the ringlike formation of DDX6 or G3BP1 and colocalization with the HCV core protein after 48 h postinfection, suggesting that the disruption of P-body formation and the hijacking of P-body and stress granule components occur at a late step of HCV infection. Furthermore, HCV infection could suppress stress granule formation in response to heat shock or treatment with arsenite (Fig. 5). In this regard, West Nile virus and dengue virus, of the family *Flaviviridae*, interfere with stress granule formation and P-body assembly through interactions with T cell intracellular antigen 1 (TIA-1)/TIAR (11). Moreover, PABP1 and G3BP1, stress granule components, are known to be common viral targets for the inhibition of host mRNA translation (34, 39). In fact, HIV-1 and poliovirus proteases cleave PABP1 and/or G3BP1 and suppress stress granule formation during viral infection (34, 39). On the other hand, HCV infection transiently induced stress granules at 36 h postinfection (Fig. 4) and did not cleave PABP1 (Fig. 6); however, HCV could suppress stress granule formation in response to heat shock or treatment with arsenite through hijacking their components around LDs, the HCV production factory (Fig. 5). Consistently, Jones et al. showed that HCV transiently induces stress granules of enhanced green fluorescent protein (EGFP)-G3BP at 36 h after infection with the cell culture-generated HCV (HCVcc) reporter virus Jc1FLAG2 (p7-nsGluc2A); however, those authors did not show the recruitment of EGFP-G3BP to LDs (18). Although we do not know the exact reason for this apparent discrepancy,

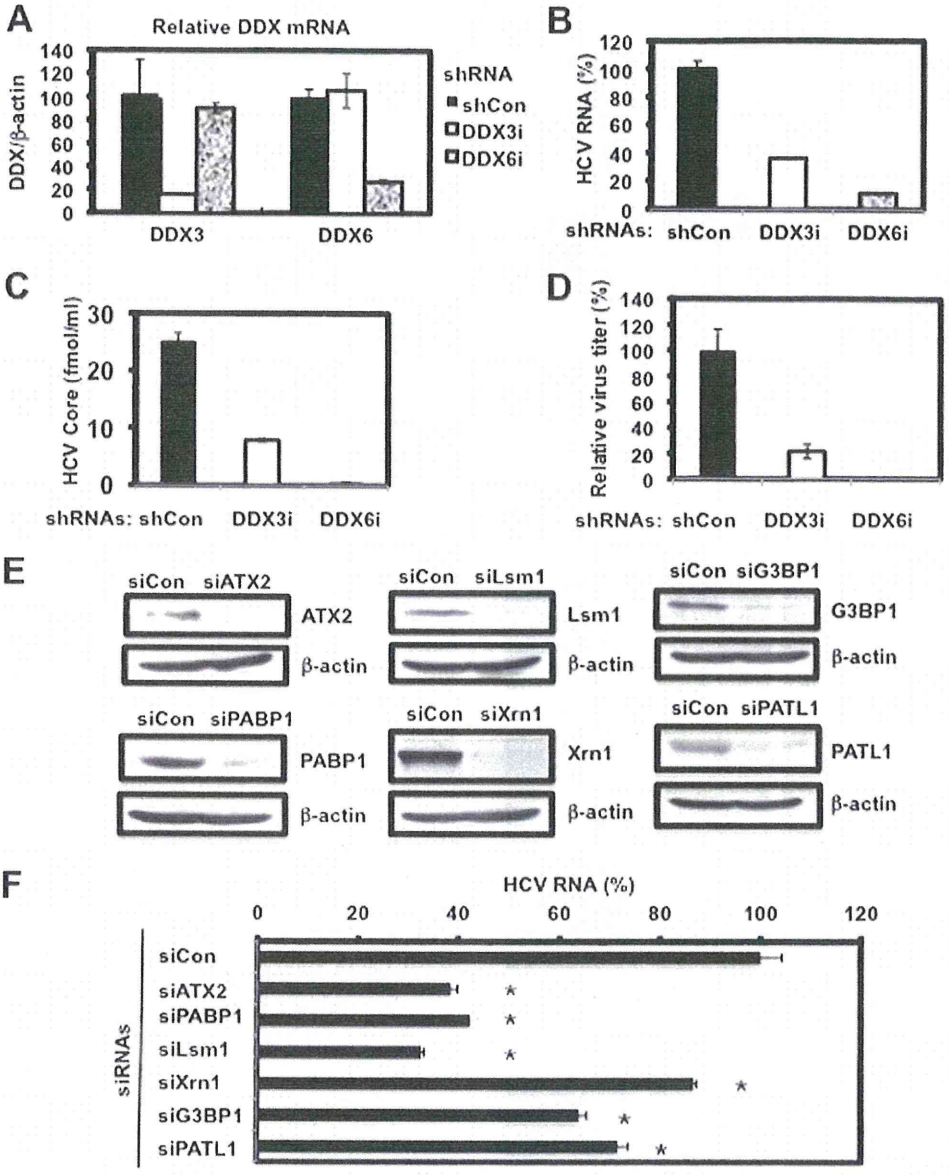

FIG. 7. Requirement of P-body and stress granule components for HCV replication. (A) Inhibition of DDX3 or DDX6 mRNA expression by the shRNA-producing lentiviral vector. Real-time LightCycler RT-PCR for DDX3 or DDX6 was also performed for β-actin mRNA in RSc cells expressing shRNA targeted to DDX3 (DDX3i) or DDX6 (DDX6i) or the control nontargeting shRNA (shCon) in triplicate. Each mRNA level was calculated relative to the level in RSc cells transduced with the control nontargeting lentiviral vector (shCon), which was assigned as 100%. Error bars in this panel and other panels indicate standard deviations. (B) Levels of intracellular genome-length HCV-JFH1 RNA in the cells at 24 h postinfection at an MOI of 4 were monitored by real-time LightCycler RT-PCR. Results from three independent experiments are shown. Each HCV RNA level was calculated relative to the level in RSc cells transduced with a control lentiviral vector (shCon), which was assigned as 100%. (C) The levels of HCV core in the culture supernatants from the stable knockdown RSc cells 24 h after inoculation of HCV-JFH1 at an MOI of 4 were determined by ELISA. Experiments were done in triplicate, and columns represent the mean core protein levels. (D) The infectivity of HCV in the culture supernatants from stable-knockdown RSc cells 24 h after inoculation of HCV-JFH1 at an MOI of 4 was determined by a focus-forming assay at 24 h postinfection. Experiments were done in triplicate, and each virus titer was calculated relative to the level in RSc cells transduced with a control lentiviral vector (shCon), which was assigned as 100%. (E) Inhibition of ATX2, PABP1, Lsm1, Xrn1, G3BP1, or PATL1 protein expression by 72 h after transient transfection of RSc cells with a pool of control nontargeting siRNA (siCon) or a pool of siRNAs specific for ATX2, PABP1, Lsm1, Xrn1, G3BP1, or PATL1 (25 nM), respectively. The results of Western blot analyses of cellular lysates with anti-ATX2, anti-PABP1, anti-Lsm1, anti-Xrn1, anti-G3BP1, anti-PATL1, or anti-β-actin antibody are shown. (F) Levels of intracellular genome-length HCV-JFH1 RNA in the cells at 48 h postinfection at an MOI of 1 were monitored by real-time LightCycler RT-PCR. RSc cells were transiently transfected with a pool of control siRNA (siCon) or a pool of siRNAs specific for ATX2, PABP1, Lsm1, Xrn1, G3BP1, and PATL1 (25 nM). At 48 h after transfection, the cells were inoculated with HCV-JFH1 at an MOI of 1 and incubated for 2 h. The culture medium was then changed and incubated for 22 h. Experiments were done in triplicate, and each HCV RNA level was calculated relative to the level in RSc cells transfected with a control siRNA (siCon), which was assigned as 100%. Asterisks indicate significant differences compared to the control treatment (*, $P < 0.01$).

several possible explanations can be offered. First, those authors examined the localization of EGFP-G3BP within 48 h postinfection, and we observed it at later times (Fig. 4). Second, they used only EGFP-tagged G3BP instead of endogenous G3BP1. Third, they used a Jc1FLAG2 (p7-nsGluc2A) clone, and an HCV-JFH1 clone could markedly induce the recruitment of the core protein to LDs compared to that of Jc1. Also, Jangra et al. failed to observe the recruitment of DDX6 to LDs at 2 days after infection with HJ3-5 virus (16). Accordingly, we also observed that most of the DDX6 still formed intact P bodies at earlier times (12 h or 24 h postinfection). Importantly, we observed the recruitment of DDX6 to LDs 48 h later (Fig. 4). Furthermore, those authors did not show the ringlike structure formation of the HJ3-5 core protein around LDs, unlike the JFH1 core protein that we used in this study. The interaction of the HCV core protein with DDX6 may explain the recruitment of P-body components to LDs. However, we do not yet know whether the P-body function(s) can be performed on LDs. At least, HCV infection did not affect the translation of several host mRNAs with 5′ caps and 3′ poly(A) tails despite the disruption of P-body formation at 72 h postinfection (Fig. 6), suggesting that HCV does not affect P-body function and that HCV recruits functional P bodies to LDs.

We need to address the potential role of stress granule components, such as PABP1, in HCV replication/translation, since the HCV genome does not harbor the 3′ poly(A) tail. Intriguingly, we have found that the accumulation of HCV RNA was significantly suppressed in PABP1 knockdown RSc cells (Fig. 7F). In this regard, Tingting et al. demonstrated previously that G3BP1 and PABP1 as well as DDX1 were identified as the HCV 3′-UTR RNA-binding proteins by proteomic analysis and that G3BP1 was required for HCV RNA replication (35). Yi et al. also reported that G3BP1 was associated with HCV NS5B and that G3BP1 was required for HCV RNA replication (42). We observed a moderate effect of siG3BP1 on HCV RNA replication (Fig. 7F). In contrast, the accumulation of HCV RNA was significantly suppressed in ATX2 and Lsm1 knockdown cells as well as in PABP1 knockdown cells (Fig. 7F), suggesting that ATX2, Lsm1, and PABP1 are required for HCV replication.

Taking these results together, this study has demonstrated for the first time that HCV hijacks P-body and stress granule components around LDs. This hijacking may regulate HCV RNA replication and translation. Indeed, we have found that the accumulation of genome-length HCV-O (genotype 1b) (14) RNA was markedly suppressed in DDX6 knockdown O cells (data not shown). More importantly, these P-body and stress granule components may be involved in the maintenance of the HCV RNA genome without 5′ cap and 3′ poly(A) tail structures in the cytoplasm for long periods, since the hijacking of P-body and stress granule components by HCV occurred at later times.

ACKNOWLEDGMENTS

We thank D. Trono for the lentiviral vector system, T. Wakita for HCV-JFH1, and K. T. Jeang for pHA-DDX3. We also thank T. Nakamura and K. Takeshita for their technical assistance.

This work was supported by a grant-in-aid for scientific research (C) from the Japan Society for the Promotion of Science (JSPS); by a grant-in-aid for research on hepatitis from the Ministry of Health, Labor, and Welfare of Japan; and by the Viral Hepatitis Research Foundation of Japan. M.K. was supported by a research fellowship from the JSPS for young scientists.

REFERENCES

1. **Anderson, P., and N. Kedersha.** 2007. Stress granules: the Tao of RNA triage. Trends Biochem. Sci. **33**:141–150.
2. **Ariumi, Y., et al.** 2003. Distinct nuclear body components, PML and SMRT, regulate the *trans*-acting function of HTLV-1 Tax oncoprotein. Oncogene **22**:1611–1619.
3. **Ariumi, Y., et al.** 2007. DDX3 DEAD-box RNA helicase is required for hepatitis C virus RNA replication. J. Virol. **81**:13922–13926.
4. **Ariumi, Y., et al.** 2008. The DNA damage sensors ataxia-telangiectasia mutated kinase and checkpoint kinase 2 are required for hepatitis C virus RNA replication. J. Virol. **82**:9639–9646.
5. **Ariumi, Y., et al.** 2011. The ESCRT system is required for hepatitis C virus production. PLoS One **6**:e14517.
6. **Beckham, C. J., and R. Parker.** 2008. P bodies, stress granules, and viral life cycles. Cell Host Microbe **3**:206–212.
7. **Bridge, A. J., S. Pebernard, A. Ducraux, A. L. Nicoulaz, and R. Iggo.** 2003. Induction of an interferon response by RNAi vectors in mammalian cells. Nat. Genet. **34**:263–264.
8. **Brummelkamp, T. R., R. Bernard, and R. Agami.** 2002. A system for stable expression of short interfering RNAs in mammalian cells. Science **296**:550–553.
9. **Chable-Bessia, C., et al.** 2009. Suppression of HIV-1 replication by microRNA effectors. Retrovirology **6**:26.
10. **Cristea, I. M., et al.** 2010. Host factors associated with the Sindbis virus RNA-dependent RNA polymerase: role for G3BP1 and G3BP2 in virus replication. J. Virol. **84**:6720–6732.
11. **Emara, M. M., and M. A. Brinton.** 2007. Interaction of TIA-1/TIAR with West Nile and dengue virus products in infected cells interferes with stress granule formation and processing body assembly. Proc. Natl. Acad. Sci. U. S. A. **104**:9041–9046.
12. **Hijikata, M., N. Kato, Y. Ootsuyama, M. Nakagawa, and K. Shimotohno.** 1991. Gene mapping of the putative structural region of the hepatitis C virus genome by in vitro processing analysis. Proc. Natl. Acad. Sci. U. S. A. **88**:5547–5551.
13. **Hijikata, M., et al.** 1993. Proteolytic processing and membrane association of putative nonstructural proteins of hepatitis C virus. Proc. Natl. Acad. Sci. U. S. A. **90**:10773–10777.
14. **Ikeda, M., et al.** 2005. Efficient replication of a full-length hepatitis C virus genome, strain O, in cell culture, and development of a luciferase reporter system. Biochem. Biophys. Res. Commun. **329**:1350–1359.
15. **Jangra, R. K., M. Yi, and S. M. Lemon.** 2010. Regulation of hepatitis C virus translation and infectious virus production by the microRNA miR-122. J. Virol. **84**:6615–6625.
16. **Jangra, R. K., M. Yi, and S. M. Lemon.** 2010. DDX6 (Rck/p54) is required for efficient hepatitis C virus replication but not IRES-directed translation. J. Virol. **84**:6810–6824.
17. **Ji, H., et al.** 2008. MicroRNA-122 stimulates translation of hepatitis C virus RNA. EMBO J. **27**:3300–3310.
18. **Jones, C. T., et al.** 2010. Real-time imaging of hepatitis C virus infection using a fluorescent cell-based reporter system. Nat. Biotechnol. **28**:167–171.
19. **Jopling, C. L., M. Yi, A. M. Lancaster, S. M. Lemon, and P. Sarnow.** 2005. Modulation of hepatitis C virus RNA abundance by a liver-specific microRNA. Science **309**:1577–1581.
20. **Jopling, C. L., S. Schütz, and P. Sarnow.** 2008. Position-dependent function for a tandem microRNA miR-122-binding site located in the hepatitis C virus RNA genome. Cell Host Microbe **4**:77–85.
21. **Kato, N., et al.** 1990. Molecular cloning of the human hepatitis C virus genome from Japanese patients with non-A, non-B hepatitis. Proc. Natl. Acad. Sci. U. S. A. **87**:9524–9528.
22. **Kedersha, N., and P. Anderson.** 2007. Mammalian stress granules and processing bodies. Methods Enzymol. **431**:61–81.
23. **Kuroki, M., et al.** 2009. Arsenic trioxide inhibits hepatitis C virus RNA replication through modulation of the glutathione redox system and oxidative stress. J. Virol. **83**:2338–2348.
24. **Kushima, Y., T. Wakita, and M. Hijikata.** 2010. A disulfide-bonded dimer of the core protein of hepatitis C virus is important for virus-like particle production. J. Virol. **84**:9118–9127.
25. **Mamiya, N., and H. J. Worman.** 1999. Hepatitis C virus core protein binds to a DEAD box RNA helicase. J. Biol. Chem. **274**:15751–15756.
26. **Miyanari, Y., et al.** 2007. The lipid droplet is an important organelle for hepatitis C virus production. Nat. Cell Biol. **9**:1089–1097.
27. **Naldini, L., et al.** 1996. In vivo gene delivery and stable transduction of nondividing cells by a lentiviral vector. Science **272**:263–267.
28. **Nonhoff, U., et al.** 2007. Ataxin-2 interacts with the DEAD/H-box RNA helicase DDX6 and interferes with P-bodies and stress granules. Mol. Biol. Cell **18**:1385–1396.
29. **Owsianka, A. M., and A. H. Patel.** 1999. Hepatitis C virus core protein interacts with a human DEAD box protein DDX3. Virology **257**:330–340.

30. **Parker, R., and U. Sheth.** 2007. P bodies and the control of mRNA translation and degradation. Mol. Cell **25**:635–646.
31. **Randall, G., et al.** 2007. Cellular cofactors affecting hepatitis C virus infection and replication. Proc. Natl. Acad. Sci. U. S. A. **104**:12884–12889.
32. **Rocak, S., and P. Linder.** 2004. DEAD-box proteins: the driving forces behind RNA metabolism. Nat. Rev. Mol. Cell Biol. **5**:232–241.
33. **Scheller, N., et al.** 2009. Translation and replication of hepatitis C virus genomic RNA depends on ancient cellular proteins that control mRNA fates. Proc. Natl. Acad. Sci. U. S. A. **106**:13517–13522.
34. **Smith, R. W., and N. K. Gray.** 2010. Poly(A)-binding protein (PABP): a common viral target. Biochem. J. **426**:1–11.
35. **Tingting, P., F. Caiyun, Y. Zhigang, Y. Pengyuan, and Y. Zhenghong.** 2006. Subproteomic analysis of the cellular proteins associated with the 3′ untranslated region of the hepatitis C virus genome in human liver cells. Biochem. Biophys. Res. Commun. **347**:683–691.
36. **Tourrière, H., et al.** 2003. The RasGAP-associated endoribonuclease G3BP assembles stress granules. J. Cell Biol. **160**:823–831.
37. **Wakita, T., et al.** 2005. Production of infectious hepatitis C virus in tissue culture from a cloned viral genome. Nat. Med. **11**:791–796.
38. **Weston, A., and J. Sommerville.** 2006. Xp54 and related (DDX6-like) RNA helicase: roles in messenger RNP assembly, translation regulation and RNA degradation. Nucleic Acids Res. **34**:3082–3094.
39. **White, J. P., A. M. Cardenas, W. E. Marissen, and R. E. Lloyd.** 2007. Inhibition of cytoplasmic mRNA stress granule formation by a viral proteinase. Cell Host Microbe **2**:295–305.
40. **Wilson, J. A., C. Zhang, A. Huys, and C. D. Richardson.** 2011. Human Ago2 is required for efficient miR-122 regulation of HCV RNA accumulation and translation. J. Virol. **85**:2342–2350.
41. **Yedavalli, V. S., C. Neuveut, Y. H. Chi, L. Kleiman, and K. T. Jeang.** 2004. Requirement of DDX3 DAED box RNA helicase for HIV-1 Rev-RRE export function. Cell **119**:381–392.
42. **Yi, Z., et al.** 2006. Subproteomic study of hepatitis C virus replicon reveals Ras-GTPase-activating protein binding protein 1 as potential HCV RC component. Biophys. Biochem. Res. Commun. **350**:174–178.
43. **You, L. R., et al.** 1999. Hepatitis C virus core protein interacts with cellular putative RNA helicase. J. Virol. **73**:2841–2853.
44. **Zufferey, R., D. Nagy, R. J. Mandel, L. Naldini, and D. Trono.** 1997. Multiply attenuated lentiviral vector achieves efficient gene delivery in vivo. Nat. Biotechnol. **15**:871–875.

Meeting Summary

Will There Be an HCV Meeting in 2020? Summary of the 17th International Meeting on Hepatitis C Virus and Related Viruses

TAKAJI WAKITA,[*] TETSURO SUZUKI,[‡] MATTHEW J. EVANS,[§] KUNITADA SHIMOTOHNO,[‖] KAZUAKI CHAYAMA,[¶] YOSHIHARU MATSUURA,[#] MAKOTO HIJIKATA,[**] KOHJI MORIISHI,[‡‡] TSUKASA SEYA,[§§] NOBUYUKI ENOMOTO,[¶¶] KAZUHIKO KOIKE,[##] NOBUYUKI KATO,[***] TATSUYA KANTO,[#] and HAK HOTTA[‡‡‡]

[*]National Institute of Infectious Diseases, Japan; [‡]Hamamatsu University School of Medicine, Japan; [§]Mount Sinai School of Medicine, New York; [‖]Chiba Institute of Technology, Japan; [¶]Hiroshima University, Japan; [#]Osaka University, Japan; [**]Kyoto University, Japan; [¶¶]University of Yamanashi, Japan; [§§]Hokkaido University, Japan; [##]The University of Tokyo, Japan; [***]Okayama University, Japan; [‡‡‡]Kobe University, Japan

Hepatitis C virus (HCV), which was discovered in 1989, is a major etiologic agent in human liver disease. Approximately 130 million people, or 2% of the population, worldwide are infected. The 17th International Meeting on Hepatitis C Virus and Related Viruses was held September 10–14, 2010, in Yokohama, Japan. The meeting was attended by almost 700 scientists from all over the world who are interested in the fundamental aspects of the molecular virology, immunology, pathogenesis, prevention, and treatment of HCV infection. Two special opening lectures given by Masaaki Komatsu and Takashi Gojobori focused attention on the related research fields of autophagy and genome biology, respectively. In the subsequent sessions, the latest research, original studies, and controversies were presented in 9 keynote lectures, 82 oral presentations, and 329 poster presentations.

Viral Entry

The opening scientific session of this meeting focused on the viral host cell entry processes. Thomas Baumert presented the keynote lecture, which included an overview of the HCV cell entry process and recent advances at his laboratory. These included the finding that HCV variants that reinfect the liver after transplantation demonstrate more efficient cell entry and are less susceptible to neutralization by host antibodies. He also described the isolation of monoclonal antibodies against claudin-1 that do not inhibit either extracellular or direct cell-to-cell HCV transfer.

Alexander Ploss described the establishment of a mouse model for studying HCV cell entry. They utilized an HCV cell culture virus (HCVcc) expressing recombinase and transgenic mice bearing a recombinase-activatable fluorescent protein. Bioluminescent imaging indicated that only mice transduced with CD81 and occludin supported HCVcc entry. The presence of an intact immune system in these animals makes it particularly important for the testing of HCV vaccine candidates. Danyelle N. Martin described a role for transferrin receptor 1 (TfR1) in mediating HCV cell entry. The inhibition of HCV entry with TfR1 antibodies and silencing, suggest this factor should be added to the growing list of cellular proteins required for HCV cell entry. Joachim Lupberger presented results from a study showing an essential role for the epidermal growth factor receptor (EGFR) in HCV cell entry. He found that EGFR is required for both mediating the interactions between two other entry factors, CD81 and CLDN1, and catalyzing the fusion activity of viral glycoproteins.

Translation/Replication

Volker Lohmann began the session by describing what is known of the functions of viral nonstructural proteins and their associated host cellular factors in viral translation and replication. He included an overview of viral isolates and model systems currently used, and presented data addressing the mechanisms for efficient replication of the JFH-1 isolate.

Several reports have focused on the molecular basis of the architecture and composition of membrane-associated sites for HCV replication, which often induce membrane alterations, such as the so-called membranous web. Brenno Wolk demonstrated that NS4B is sufficient to direct all nonstructural proteins into the viral replication complex compartment, and that intragenotype-specific interactions are required for NS4B-dependent recruitment of NS5A. Ines Romero-Brey showed that the membranous web predominantly contains double-membrane vesicles with various diameters. These vesicle structures were connected to the endoplasmic reticulum (ER) through funnel-like structures.

Several DDX DEAD-box RNA helicases were identified as host factors associated with HCV replication. Yasuo Ariumi presented the cross-talk of HCV with DDX proteins and the role of distinct DDX proteins in viral replication. Tetsuro Shimakami and Selena M. Sagan reported the importance of miR-122 to not only enhance IRES-mediated translation, but stabilize positive-strand HCV RNA by binding to its 5′ extremity. Enzymatic activity of host phosphatidyl-inositol-4 kinase III alpha was shown to be critically involved in HCV replication and the activity is regulated by HCV NS5A (Simon Reiss). Nam-Joon Cho reconstituted a functionally active full-

0016-5085/$36.00
doi:10.1053/j.gastro.2011.05.027

length HCV polymerase on a biomimetic membrane platform. Deborah Harrus found that guanosine triphosphate specifically stimulates the initial step of de novo initiation by stimulating transition of newly formed linker primer.

Assembly and Release

In the keynote lecture, Guangxiang G. Luo presented an overview of particle assembly and release, and the impact of apolipoprotein (Apo) E in the entry and assembly of HCV. He demonstrated the inhibition of HCVcc entry by treatment with anti-ApoE antibody and the direct interaction of ApoE with NS5A.

Ann L. Wozniak showed an important role for p7 in the production of infectious particles. Their data suggest that p7 stimulates virus production through the alkalization of intracellular vesicles. Ophelia Granio showed that both p7 and NS2 are required for the recruitment of core from lipid droplets (LDs) to ER. Costin-Ioan I. Popescu showed that NS2 accumulated in dotted structures in the ER in juxtaposition with Core and LDs. They concluded that cross-talk among Core, E1, E2, p7, and NS2 was essential for virion assembly. Vlastimil Jirasko demonstrated point mutations in the transmembrane regions of NS2 impaired the particle production and suggested that NS2 serves as a platform of viral and cellular proteins that coordinates HCV assembly. Qisheng Li identified the proviral function of IKKα by genome wide siRNA screening. IKKα regulates lipid metabolism and biogenesis of LDs and may enhance production of virus particles. The very low-density lipoproteins are secreted via a Golgi-dependent pathway. Bryan R. Bishe demonstrated the important role of phosphatidylinositol-4-phosphate and its interacting protein GOLPH3 in HCV secretion in the trans-Golgi network. Roland Remenyi showed 3-dimensional visualization of the HCV life cycle in cultured cells by electron tomography. They detected virus-like particles at various cytoplasmic locations. Viral particles in the proximity of LDs and within sponge-like inclusion were observed. These results provide ultrastructural visualization of putative assembly sites close to LDs.

Host Factors

In the invited lecture, Sara Cherry presented an overview of high-throughput screening toward the identification of host factors required for viral infection.

The contribution of autophagy to the HCV life cycle was also presented in this section, most notably, host factors linked with lipids. Tsubasa Munakata showed that the fatty acid synthase is required for efficient HCV replication. They also suggested the importance of palmitate for HCV replication. Samantha L. Blackham presented both the thioredoxin-interacting protein and the peroxisome proliferator activated receptor-α have significant effects on HCV replication. The host factors functioning on infectious HCV particle production were also reported. Takayuki Hishiki demonstrated the isoform dependent binding affinities of ApoE for low-density lipoprotein receptors and they affect infectivity of HCV. Laurent Chatel-Chaix found that Y-box binding protein interacted with HCV NS3 protein and viral RNA and was relocalized from nucleocytoplasmics site to the core-containing surface of LDs. Mohsan Saeed reported that the ER-associated degradation pathway was activated by HCV infection in a viral envelope protein-dependent manner. Po-Yuan Ke showed that HCV infection induces the unfolded protein response and activates the autophagic pathway. They proposed that autophagy contributes to the suppression of HCV in an autolysosome formation-dependent manner. Hiroto Kambara did not find any effects on HCV replication by inhibition of autophagosome formation in replicon cells. They proposed a role for autophagy induced by HCV infection to avoid the generation of vacuolation harmful to cell survival. Qisheng Li reported the network map of cellular pathways and machineries that are associated with HCV life cycle.

Very low-density lipoprotein is now considered to be one of a component of HCV particles. LDs are composed of fatty acid, triglyceride, and cholesterol, surrounded by several types of lipoproteins. In addition, Daniel J. Felmlee reported that chylomicron-associated viruses may be generated by virion association while in the vascular compartment. Francois Jean showed that the serine protease inhibitor protein Spn4A was modified to be directed to Site-1 protease specifically and was introduced into adenovirus vector to inhibit cholesterol and fatty acid syntheses for down-regulation of HCV propagation. The modified serpin could suppress Site-1 protease activity, reduce the LD, and block HCVcc infection. Nicolas Menzel tried to identify novel cellular factors involved in HCV assembly and release and found ERK inhibitor and cytosolic phospholipase A2 (cPLA2) inhibitor reduce viral production. cPLA2 inhibitor also reduced the amount of LD-associated core and supernatant ApoB/E. cPLA2 may be crucial for assembly of infectious HCV particles, possibly through participating in the formation of lipoproteins. Kohji Moriishi reported that the proteasome activator PA28γ participates in HCV propagation. PA28γ may participate in the propagation of HCV by regulating the degradation of Core in both ubiquitin-dependent and -independent manners. NS5A is regulated by phosphorylation of several host protein kinases. Takahiro Masaki identified 79 serine threonine protein kinases that were tightly associated with NS5A. Two of these may regulate the production of viral particles and/or viral replication.

Innate Immunity

The early phase of host defense against viral infection has largely been delineated based on recent advances in innate immunity. In the invited lecture, Manoj N. Krishnan introduced his comprehensive study on the Toll-like receptor 3–TRIF (TICAM-1) pathway. Using RNAi and polyI:C, he screened the genes specifically up-regulated via the TRIF (TICAM-1) pathway. He expected that some viral infections are selectively blocked by the IPS-1 pathway, while others are blocked by the TRIF pathway.

Michael Gale, Jr., identified IFITM1 inhibits HCV infection. IFITM1 assembles with CD81 and tranlocates to the tight junction. This translocation of CD81 hampers the receptor function of CD81. They also discovered a novel pathway for ISGF3 activation. A non-receptor type tyrosine kinase-1 triggers activation of ISGF3 independent from the classical IFNAR pathway. IP-10 is a chemokine and is a negative predictor for pegylated interferon (IFN)/ribavirin therapy. Matthew L. Albert indicated that there is a 2-amino-acid–deleted form of IP-10 that serves as an antagonist for intact IP-10, and this form abrogates an early virologic response. As this IP-10 truncation is mediated by dipeptidylpeptidase IV, they believed that dipeptidylpeptidase IV is a novel therapeutic target for HCV patients during IFN therapy. Joo Chun Yoon suggested that activation of natural killer cells is inhibited by HCV-infected hepatocytes. They claimed that the early phases of HCV infection may be established through the failure of virus-inducible natural killer cell activation. Shin-ichiro Nakagawa reported that polyI:C induces both type I IFN and IFN-λ in human hepatocytes. The antiviral effect appears to parallel the induction of IFN-λ. This, together with the report by Emmanuel Thomas, suggests that the IFN-λ system is activated in HCV infected hepatocytes.

Adaptive Immunity

In a keynote lecture, Robert Thimme summarized the mechanisms of HCV-induced T-cell dysfunction. Multifaceted factors contribute to the hyporesponsiveness of T cells, including viral mutations, primary T-cell failure, lack of support from dendritic cells, expression of inhibitory molecules on T cells, and abundance of regulatory T cells (Tregs). Whether the ability of HCV-specific CTLs is comparable with that of CTLs having other specificities remains controversial. Bianca Seigel showed that HCV-specific CTLs are functionally impaired when compared with other CTLs, irrespective of their expression of inhibitory receptors or differentiation stages. CD161 is a C-type lectin that is expressed in HCV-specific $CD8^+$ T cells with tissue homing phenotype. Vicki M. Fleming found that $CD4^+CD161^+$ T cells produce large amounts of inflammatory cytokines and accumulate in the liver, where they are thought to exert pro-inflammatory roles. Naruyasu Kakita reported that certain adaptive Tregs, known as interleukin (IL)-10–producing type 1 Tregs, are increased in HCV-positive hepatocellular carcinoma patients, and their significance in hepatocellular carcinoma was greater than that of natural Tregs. Even in patients who have attained a sustained virologic response, trace amounts of HCV RNA are sporadically detectable in plasma. Barbara Rehermann reported the inoculation studies of such plasma. Residual HCV RNA in patients was able to infect chimpanzees and induced broad, HCV-specific T-cell responses. HCV RNA levels continued to be high when T-cell responses declined, suggesting that such HCV remains transmissible as hepatotropic pathogens.

Pathogenesis

In the invited lecture, Michael Diamond presented new mechanisms for West Nile virus immune evasion via 2'O methylation of viral RNA to subvert host innate immunity.

Genome-wide analysis of quantitative data (transcriptomics, proteomics, and metabolomics) facilitates systems biology analysis of HCV infection. Deborah L. Diamond analyzed the pathways involved in the progression of chronic hepatitis, namely, fibrosis and carcinogenesis, and found that molecules relating to cell metabolism including fatty acid oxidation enzymes and antioxidant systems may be master regulators of liver disease progression in HCV infection. HCV core protein has been shown to play a key role in the development of steatosis in HCV infected liver, especially in patients with genotype 3a HCV infection. Sophie Clement-Leboube showed that PTEN expression was down-regulated in the HCV infected liver. Analysis of lipo-viral-particle from hepatitis C patients by Olivier Diaz revealed that empty lipo-viral-particle lacking HCV RNA outnumbers those with RNA. The presence of virus-modified lipoproteins in HCV-infected patients may play a role in the pathogenesis of hepatitis C. Massimiliano Pagani used serum miRNA signatures to monitor liver disease in HCV infection and found miRNome candidates that are specific for HCV disease progression. Shuhei Taguwa showed that Con1 replicon induces incomplete autophagy through the dysfunction of autolysosomal acidification, which results in the secretion of immature cathepsin B in cells. Because the secretion of the protein is enhanced in many types of tumors, this observation may be associated with the pathogenesis of liver tumorigenesis in HCV infection.

The existence of extrahepatic manifestations is another issue of interest. Essential mixed cryoglobulinemia, membranoproliferative glomerulonephritis, and Sjögren syndrome are conditions that have been shown to correlate

with HCV infection. Nicola A. Fletcher reported that brain microvascular endothelial cells express all the recognized entry factors for HCV, and brain microvascular endothelial cells actually support infection by HCVpp and HCVcc. This suggests potential disorders of the central nervous system in HCV infection.

Treatment

In the keynote lecture, Masashi Mizokami presented "Genome-wide association study and its application for HCV treatment." He emphasized that the functional relevance of IL-28B single nucleotide polymorphisms should be elucidated to further advance the progress of research on the mechanisms of chronic HCV infection and treatment.

Yasuhiro Asahina presented that genetic variation in IL-28B is associated with gene expression involving innate immunity. Minor alleles of IL-28B, as well as a higher RIG-I/IPS-1 ratio are associated with null viral response. Martin Laggins correlated IL-28B genetic variation with pretreatment levels of IP-10 and HCV RNA throughout therapy. The favorable genetic variation of IL-28B single nucleotide polymorphisms (major allele) was significantly associated with lower baseline IP-10. Masao Honda revealed that hepatic IFN-stimulated genes (ISGs) are associated with genetic variation in IL-28B and the outcome of IFN therapy for chronic hepatitis C using microarray gene expression profiling of the biopsied liver samples. Multivariate logistic regression analysis showed that ISGs, fibrosis stage, and ISDR mutations were strongly associated with viral response. Hepatic ISGs were associated with the IL-28B polymorphism and expression was significantly higher in patients with the minor genotype than in those with the major genotype. Takashi Motomura also analyzed ISG expression using liver transplantation samples. Expression of ISGs in recipients' liver carrying the minor allele of IL-28B was significantly up-regulated when compared with the major allele. Surprisingly, IFN sensitivity for recurrent hepatitis C after liver transplantation is influenced by IL-28B genetic variation not only in recipients, but also in donors.

Drug Development

This session opened with a keynote lecture by Raffaele De Francesco describing the current state of drug development for patients with chronic hepatitis C. Because of the rapid development of NS3/4A, NS5A, and NS5B inhibitors, he finally presented the hopeful message "Will there be an HCV meeting in 2020?".

Lotte Coelmont characterized an NS5A D320E variant showing low-level resistance to DEB025, a cyclophilin (Cyp)-binding molecule. This study suggests that DEB025 presents a high barrier to resistance, and that D320E confers low-level resistance to DEB025 by reducing the need for CypA-dependent isomerization of NS5A. Paul Targett-Adams reported that NS5A inhibitors stimulated redistribution of NS5A from the ER to ring-like structures in the cytoplasm, and disrupted colocalization with NS5B. This study suggests that NS5A inhibitors perturb formation of new replication complexes rather than acting on preformed complexes. Luis M. Schang developed a family of small synthetic rigid amphiphiles with large hydrophilic heads and small, planar and rigid hydrophobic tails, called RAFIs (rigid amphipathic fusion inhibitors), which inhibit the infectivity of enveloped virions including HCV. Emmanuel Thomas screened host genes involving the anti-HCV activity of ribavirin. Among 64 host genes, several candidate genes were identified as host factors involving ribavirin's anti-HCV activity. Interestingly, silencing of the *ITPA* gene increased the anti-HCV activity of ribavirin. Pablo Gastaminza identified a novel family of 1,2-diamines as an anti-HCV reagent from a chemical library. The analysis of ~300 derivatives identified several compounds with enhanced potency and low cytotoxicity.

Vaccines/Epidemiology

HCV therapeutic vaccines are aimed to induce effective T-cell responses. Marianne Mikkelsen reported that vaccination of mice with recombinant adenovirus expressing HCV NS3 fused to the MHC class II chaperon protein invariant chain significantly enhanced NS3 specific $CD8^+$ T-cell responses, and protected mice against NS3-expressing vaccinia virus challenge. This vaccination induced polyfunctional $CD8^+$ memory T cells. Lars Frelin aimed to restore immunologic function through vaccination in a transgenic mouse model with impaired HCV-specific T-cell responses owing to a persistent presence of hepatic HCV NS3/4A antigens. They found that heterologous sequences improved activation and expansion of NS3/4A-specific T cells in a wild-type host, as well as in a tolerant NS3/4A-transgenic mouse model. The authors also suggested an important role for Tregs in the impaired HCV-specific T-cell responses.

Livia M.G. Rossi examined antibody cross-immunoreactivity against different HVR1 variants to identify antigens with a possible application of HCV vaccine development. The authors identified a small set of HVR1 variants that cross-immunoreacted with a large number of HVR1 peptides, thus suggesting their potential use in the development of HCV vaccine candidates.

Conclusion

HCV2010 in Yokohama was successful and contributed to the progress of research in the field. HCV infection remains one of the most serious worldwide health problems. The goals of this symposium were to

increase the scientific understanding of this virus and gain insights applicable to future efforts to control its infection. From this point of view, we gained further fundamental understanding about HCV at the meeting. The discovery of IL-28B as a new host factor involved in HCV treatment and pathogenesis had a major impact on HCV research. New treatment advances have been made in recent years and will continue in the near future. We would like to conclude that this meeting was successful in providing opportunities for exchanging up-to-date information and international collaboration. The next meeting will take place in Seattle, Washington, from September 8–12, 2011 (http://www.hcv2011.org/).

Reprint requests

Address requests for reprints to: Takaji Wakita, MD, PhD, Department of Virology II, National Institute of Infectious Diseases, 1-23-1 Toyama, Shinjuku-ku, Tokyo 162-8640, Japan. e-mail: wakita@nih.go.jp; fax 81-3-5285-1161.

Conflicts of interest

The authors disclose no conflicts.